

"RADIATION INDUCED HETEROGENEOUS CATALYSIS. EXPERIMENTAL
STUDY OF THE RELATIONSHIP BETWEEN BAND GAP
OF SOLIDS AND WATER DECOMPOSITION IN A
GAMMA RADIATION FIELD."

BY

GEORGE R. GOEBEL

ProQuest Number: 11016519

All rights reserved

INFORMATION TO ALL USERS

The quality of this reproduction is dependent upon the quality of the copy submitted.

In the unlikely event that the author did not send a complete manuscript and there are missing pages, these will be noted. Also, if material had to be removed, a note will indicate the deletion.



ProQuest 11016519

Published by ProQuest LLC (2019). Copyright of the Dissertation is held by the Author.

All rights reserved.

This work is protected against unauthorized copying under Title 17, United States Code
Microform Edition © ProQuest LLC.

ProQuest LLC.
789 East Eisenhower Parkway
P.O. Box 1346
Ann Arbor, MI 48106 – 1346

SUBMITTAL SHEET

A Thesis submitted to the Faculty and the Board of Trustees of
the Colorado School of Mines in partial fulfillment of the requirements
for the degree of: Master of Science in Physics

Signed: George R. Guebel
Student

Golden, Colorado

Date: Dec. 18, 1978

Approved: Wm B. Law
Thesis Advisor

W. Schouergast
Head of Department

Golden, Colorado

Date: Dec 18, 1978

ABSTRACT

A relationship between the band gap of solids and water decomposition in a gamma radiation field, occurring from the catalytic activity due to electron-hole recombination, is tested. Solids with band gaps between 2.34 ev and 7.77 ev are suspended in a vessel containing water which is placed in a gamma radiation environment. A maximum in water decomposition (or molecular hydrogen yield analyzed by a gas chromatograph) is detected using SnO_2 whose band gap is 4.3 ev. Experimental results indicate the maximum radiation catalytic decomposition of water occurs when the solid has a band gap between 3.0 ev and 5.5 ev. This coincides with the 4.97 ev bond energy necessary to break the O-H bond of the water molecule.

DEDICATION

This paper is dedicated to my entire family, especially my wife Carol, my son George, my mother Bertha and my Grandmother Bertha. Their endurance and helpfulness has been overwhelming.

This paper is especially dedicated to my father, George S. Goebel, who died July 3, 1974.

ACKNOWLEDGEMENTS

The experimental work was conducted at the Veterans Administration Hospital, Denver, Colorado. I would like to express my appreciation for the use of their Gammacell and for their cooperation.

I would like to thank the DOE from which the funds were made available for the experimental research.

Appreciation is extended to my committee members: Dr. Law, Dr. Morse, Dr. Copeland and Dr. Williamson, whose knowledge and advice led to the completion of my Master thesis.

A special thanks to my wife Carol who typed and retyped this paper.

TABLE OF CONTENTS

	<u>Page</u>
ABSTRACT	ii
DEDICATION	iii
ACKNOWLEDGEMENTS	iv
LIST OF TABLES	vi
LIST OF FIGURES	vii
INTRODUCTION	1
THEORY	5
EXPERIMENTAL DESIGN	11
PROCEDURE	22
FLUX MEASUREMENTS OF THE GAMMA CELL	24
CALIBRATION OF GAS CHROMATOGRAPH AND INTEGRATOR	28
CALIBRATION OF FLOW METER	30
EXPERIMENTAL RESULTS	34
DISCUSSION OF RESULTS	39
CONCLUSION AND RECOMMENDATIONS FOR FUTURE WORK	41
APPENDIX I - GRAPHS OF EXPERIMENTAL DATA	44
APPENDIX II - TABULATION OF EXPERIMENTAL DATA	59
BIBLIOGRAPHY	75

LIST OF TABLES

	<u>Page</u>
1. SOLIDS USED AS CATALYSTS	4
2. ABSORBANCE VALUES	26
3. DOSE RATE VALUES	26
4. CHANGE IN RADIATION DOSE WITH TIME	27
5. RESULTS OF CALIBRATION GAS RUNS	29
6. CALIBRATION OF FLOW METER	32
7. RADIATION CATALYSIS TESTS	36
8. VALUES FOR n_H , ppm, $G_{(H_2)}$, FOR THE CATALYSTS	37
9. EXPERIMENTAL DATA	59

LIST OF FIGURES

	<u>Page</u>
1. DIRECT BAND GAP TRANSITIONS	8
2. INDIRECT BAND GAP TRANSITIONS	9
3. EXPERIMENTAL SETUP	12
4. AUTOMATION OF INTEGRATOR	14
5. DIFFERENTIAL FLOW CONTROLLER	16
6. TYPICAL H ₂ PEAK	18
7. RADIATION VESSEL	19
8. RADIATION VESSEL SUPPORT	20
9. SOAP BUBBLE METER	31
10. ACTUAL FLOW RATE vs MEASURED FLOW RATE	33
11. BAND GAP OF SOLID CATALYSTS vs AVERAGE INTEGRATOR COUNTS	38
12. BAND GAP OF SOLID CATALYSTS vs PPM	43
13. RUN #127 - H ₂ O + MoO ₃	45
14. RUN #121 - H ₂ O + MoO ₃	46
15. RUN #134 - H ₂ O + In ₂ O ₃	47
16. RUN #138 - H ₂ O + TiO ₂	48
17. RUN #120 - H ₂ O + TiO ₂	49
18. RUN #128 - H ₂ O + V ₂ O ₅	50
19. RUN #137 - H ₂ O + MgO	51
20. RUN #119 - H ₂ O + MgO	52
21. RUN #136 - H ₂ O + Sb ₂ O ₃	53
22. RUN #131 - H ₂ O + HfO ₂	54
23. RUN #130 - H ₂ O + SnO ₂	55
24. RUN #139 - H ₂ O	56
25. RUN #132 - H ₂ O	57
26. RUN #118 - H ₂ O	58

INTRODUCTION

Radiation induced heterogeneous catalysis is the process which increases the rate of chemical reactions in fluids in the presence of a solid surface or solid catalyst in a radiation environment. An electronic theory of catalysis suggests that heterogeneous catalytic activity occurs from the recombination of the electron and hole formed when a solid catalyst is irradiated (1). Recombination of the electron and hole creates a photon whose energy is normally equal to the width of the forbidden band gap (E_g). The photon energy is released directly to the adsorbed fluid molecule. If the photon energy is greater than the bond energy (U) of the adsorbed fluid molecule the bond should break and a radiation induced heterogeneous catalysis reaction occurs. Radiation induced heterogeneous catalysis reactions may occur if $E_g \leq U$, since the photon emitted from the electron hole recombination may be greater than the band gap.

Related Work

1. Cockelbergs et al (2) suggested the possibility of an energy transfer mechanism for that which is adsorbed by the solid substrate and is then transferred to the adsorbed reactants.
2. Krylov (1) investigated the connection between catalyst activity of certain solid oxides and the width of their forbidden band gaps in the dehydrogenation of alcohols. Some of the solid oxides were semi-conductors and others were electrical insulators. Some correlation between band gap and catalyst activity was observed. Krylov suggested that under conditions of continuous formation and annihilation of electron-hole pairs, the system is not in a state of thermodynamic equilibrium. Krylov explained this by

suggesting a relationship involving the Fermi levels of solids. He also suggested that through recombination of free electrons and positive holes formed during radiation absorption, photon energy is released directly to the adsorbed species. This photon energy is equivalent in magnitude to the value of the band gap. If this is greater than the band energy of the adsorbed molecule, the bond will rupture.

3. Klissurski (3) related the bond energies in certain metal oxides with their band gap energies and their catalytic activity. His data includes only oxides with small band gap energies.

4. Morse (4) synthesized ammonia and oxides of nitrogen by irradiating aerated water containing suspended solids. An improvement in yield was shown when suspended solids whose band gaps were close to the energy of the N_2 bond were used.

Experimental Concept

An experimental relationship between the band gap of certain solids and the decomposition of the adsorbed fluid molecules in a radiation environment is studied. To support the concept of radiation induced heterogeneous catalysis, decomposition of water is used as an indication of the performance of the solid catalysts. This concept is tested by the comparison of molecular hydrogen yield from irradiated water with a solid powder catalyst compared with irradiated water with no catalyst (baseline data) present.

The bond energy of a water molecule is determined by the following method (5). The heat of formation of water is 220 kcal/mole or 9.57 ev/molecule. Since the water molecule consists of two O-H bonds, the bond energy E_{O-H} should equal approximately one half of this value. Then $E_{O-H} = 4.79$ ev/molecule.

Powdered solids, whose band gaps are bracketed around the bond energy of the water molecule, are suspended by a flow of nitrogen gas in a vessel containing water. The vessel is placed in a Co⁶⁰ Gammacell. An increase in the amount of hydrogen molecules caused by the decomposition of the water molecules should be evident when the band gap of the solid is near the bond energy of the water molecule. The hydrogen yield is measured by a gas chromatograph.

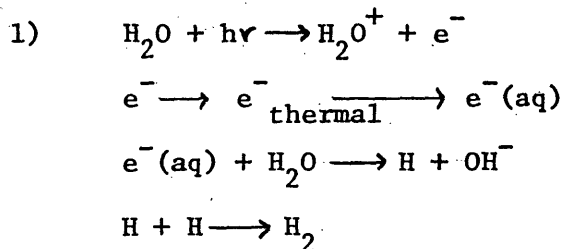
Catalyst selection is based on the band gap of the solid and its availability. With a calculated E_{O-H} energy of 4.79 ev/molecule, solids with band gaps from 2.34 ev to 7.77 ev are used (6). Table 1 lists the solids and their band gaps used in this experiment.

SOLID	BANDGAP
V_2O_5	2.34 eV
In_2O_3	2.619 eV
MoO_3	2.8 eV
TiO_2	3.0 eV
Sb_2O_3	3.31 eV
SnO_2	4.3 eV
HfO_2	5.55 eV
MgO	7.77 eV

Table 1: Solids Used as Catalysts

THEORY

Gamma rays with energies of 1.33 and 1.17 Mev from a Co^{60} source, interacting with water molecules, produce Compton electrons with maximum energies of 1.12 Mev. The maximum electron energy will occur when a 1.33 Mev gamma ray interacts with an electron and the created secondary photon emerges in the opposite direction of the incident photon. These electrons lose energy, mainly by inelastic collisions with the water molecules, and become thermalized and hydrated ($\bar{e}(\text{aq})$). (A hydrated electron (7,8) is a thermal electron which polarizes the surrounding molecules and orientates the water dipoles, to create a small potential well. The hydrated electron becomes trapped in the potential well and eventually reacts with a water molecule.) The water molecules decompose in the presence of ionizing radiation and molecular hydrogen is formed, generally by the following mechanism (7,9,10).



The number of H_2 molecules produced per 100 ev of energy deposited in pure water is denoted as $G(\text{H}_2)$ and has a value of 0.45 (9). This value is fairly independent of the linear energy transfer of the radiation source, of its dose rate, and of the pH value of the water.

If 100 grams of pure water are exposed to a Co^{60} gamma radiation source, the amount of molecular hydrogen produced (N) in cc/min can be calculated by the following equation:

$$2) \quad N = \frac{D G(H_2)}{A}$$

where: $D = \text{dose rate } \frac{\text{ev}}{\text{gram.minute}}$

$$G(H_2) = 0.45$$

$A = 2.68 \times 10^{19}$ molecules/cc (Number of molecules/cc of a gas at standard conditions. Derived from Avogadro's number).

With a dose rate (D) of 10^6 rads per hour (1 rad = 6.24×10^{13} ev/gram), 0.017 cc/min of molecular hydrogen will be produced under standard conditions. Thus there is an inability to generate high yields of molecular hydrogen from the irradiation of pure water.

The band theory of solids suggests that the valence and conduction bands of semiconductors and insulators are separated by a forbidden band gap of energy E_g (Figure 1). A solid with a direct band gap has the conduction band minimum and valence band maximum at the same location in k space (11,12). A solid with an indirect band gap is one whose conduction band minimum and valence band maximum occur at different positions in k space (Figure 2).

A photon of energy $E \geq E_g$ interacting with the solid can cause an electron-hole pair combination causing an electron to move from the valence band to the conduction band. An electron-hole recombination will ensue with a release of a photon (12), normally with an energy equivalent to the band gap E_g . (Based on density of available states).

In a direct band gap solid, the photon emitted by the electron-hole recombination will usually have an energy equal to the band gap. Other transitions may also occur where the photon energy is greater than the band gap. (Transitions may occur at other places in k space besides the position of the band gap, see Figure 1).

A solid with an indirect band gap may have an electron-hole recombination at the same location in k space emitting a photon with energy greater than the band gap. A transition in k space between the minimum of the conduction band and the maximum of the valence band, located at different places in k space, can occur with the creation of a photon and a creation or annihilation of a phonon. (Conservation of wave vector, Figure 2). Thus photon energies other than the band gap energy may be obtained.

Excitation by Co^{60} gamma ray (energies, 1.17 and 1.33 mev) interact and cause electron-hole pairs. These electron-hole pairs recombine with the emission of a photon of energy usually equal to the energy of the forbidden band gap.

Radiation induced heterogeneous catalysis is the process which increases the rate of chemical reaction in fluids in the presence of a solid surface or solid catalyst in a radiation environment. Heterogeneous catalysis reactions occur in three basic stages: adsorption, reaction, and desorption (13,14).

The fluid (water) is chemisorbed on the surface of the solid powder forming a weak chemical bond.

Gamma rays from the Co^{60} source create electron-hole pairs in the solid powder. The electron-hole pairs recombine with the emission of a photon which normally has an energy equivalent to the band gap of the solid. This photon can be released directly to the adsorbed water molecule. If the energy is greater than the bond energy of the water molecule (4.79 ev), the bond should break.

The broken molecule, H and OH, is then desorbed from the surface.

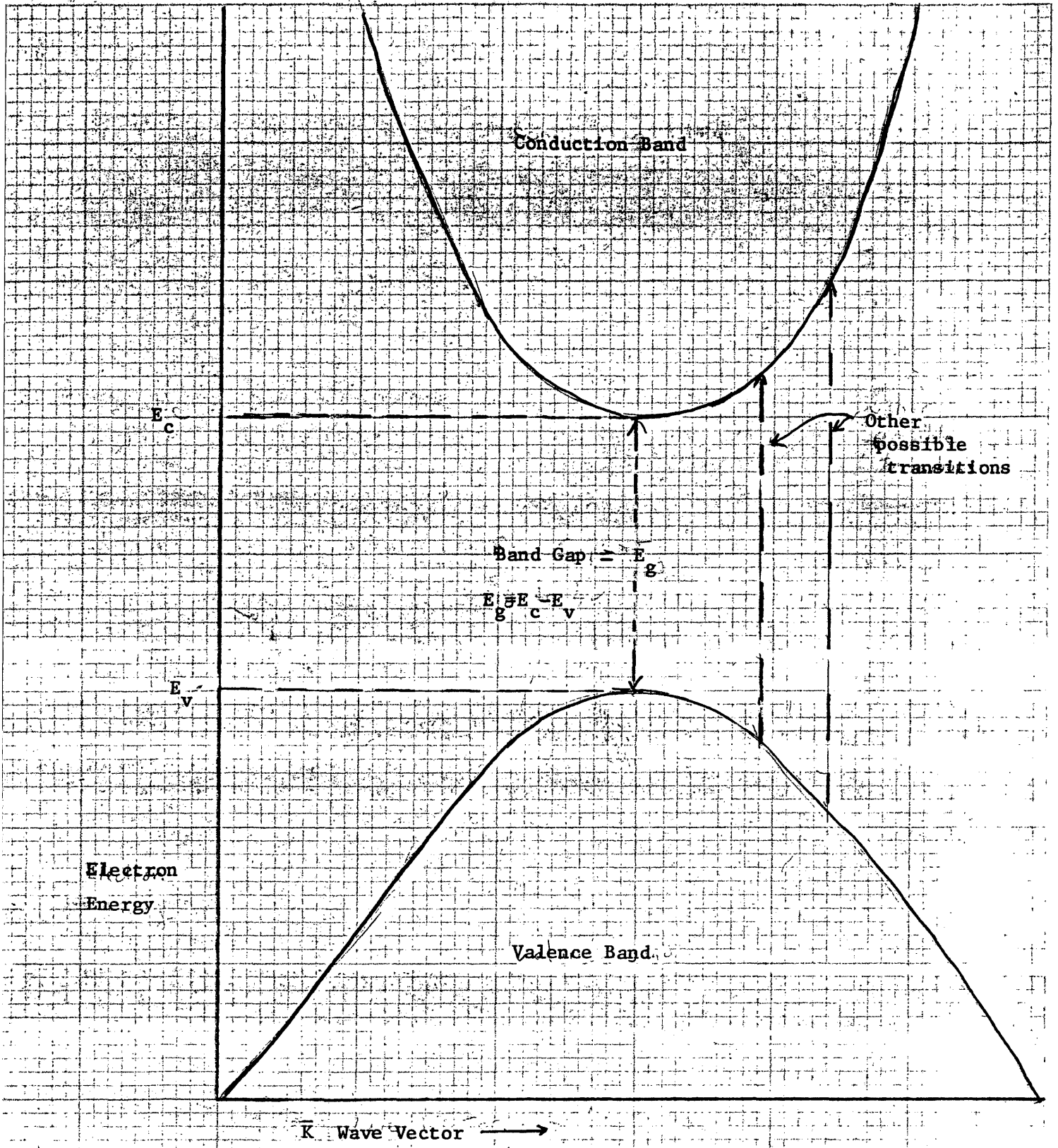


Figure 1 Direct Band Gap Transitions

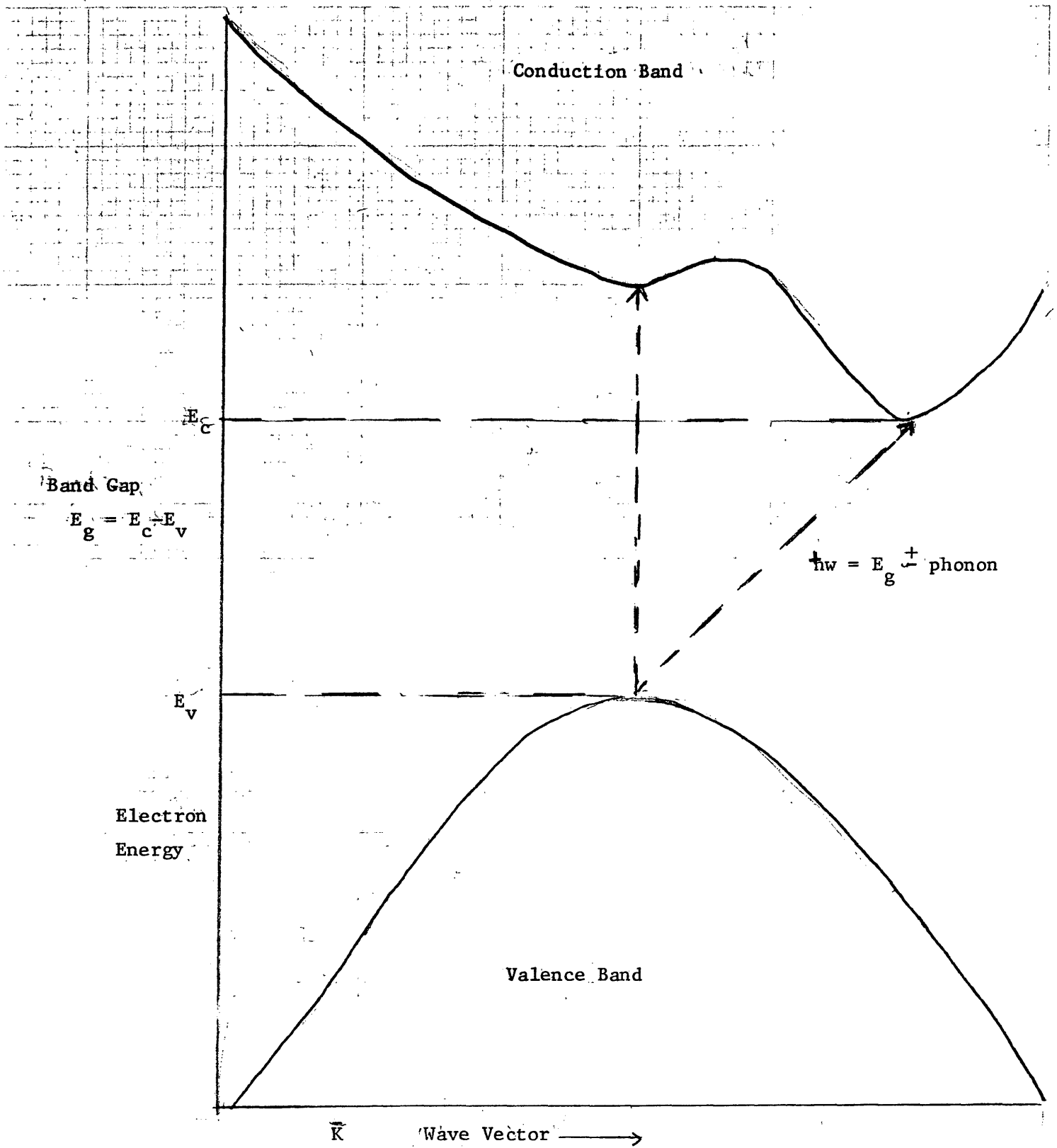
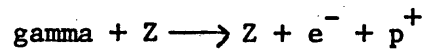
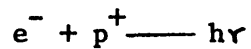


Figure 2. Indirect Band Gap Transitions.

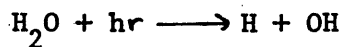
Radiation induced heterogeneous catalysis with water as the adsorbed species and Z as the solid catalyst can be summarized as follows:



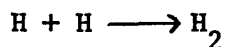
electron-hole generation



electron-hole recombination



H₂O bond breakage



Desorption and hydrogen molecule formation

EXPERIMENTAL DESIGN

Deionized water (specific resistivity approximately 2 megohm/cm) and a solid in powder form are contained in a specially designed glass vessel which is placed in a gamma radiation field. The transport gas, high purity (99.995%) dry grade nitrogen, is bubbled through the water to suspend the catalyst and to transport any hydrogen generated by radiation induced catalysis, to a gas chromatograph for analysis. The experimental setup is shown in Figure 3.

Apparatus

1. Gas Chromatograph:

A Carle analytical gas chromatograph Model #111 with automatic sampler is used for the detection of hydrogen. A six foot molecular sieve 5A 45/60 column is used for the analytical column. The carrier gas is high purity dry grade nitrogen with a purity of 99.995%. The nitrogen pressure is 17 psi which produces a flow rate of approximately 10 cc/min. The columns and detector in the gas chromatograph are kept at a constant temperature of 40°C by a full proportional temperature controller. The carrier gas flow rate and temperature setting determines the time which the gas chromatograph detects the hydrogen. Control settings are the same for all runs and are as follows:

Readout -- left column
Bridge setting - thermistor
Output - 1024
Temperature - 40°C
Inlet Δ T - off
Power - on

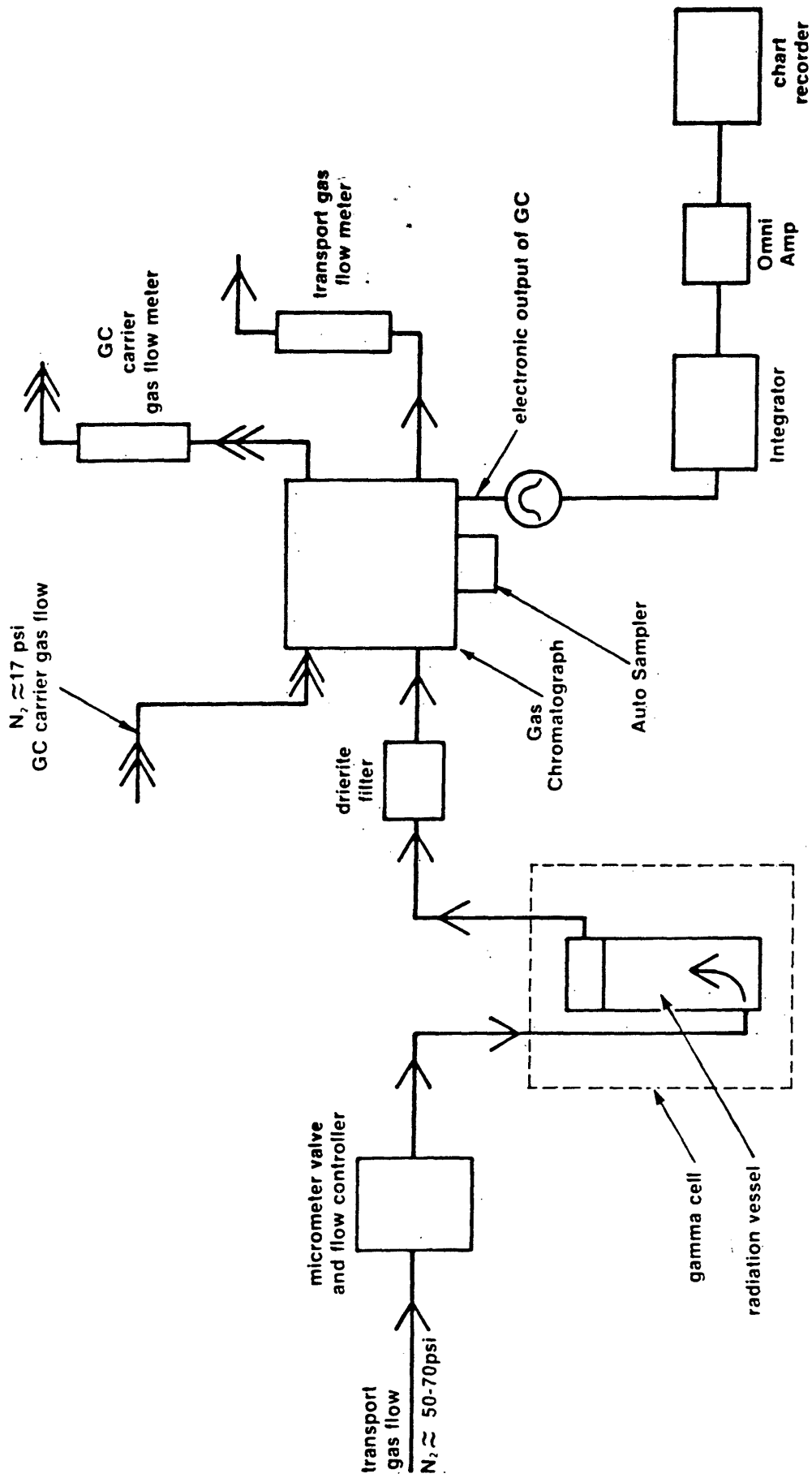


Figure 3 — Experimental Setup

The auto sampler part of the gas chromatograph allows automatic sampling of the transport gas at a maximum of one hour intervals. Auto sampling of most runs are done at 30 minute intervals for a period of five minutes each. Relay RY2, see Figure 4, contains three unused contacts which are used to automate the integrator.

2. Digital Integrator:

A digital integrator made by Columbia Scientific Industries Model Number CSI-38 is used to determine the absolute number of hydrogen molecules. The integrator produces a count = $\int_{T_1}^{T_2} (V_{GC} - V_{BC}) dt$ where T_1 and T_2 are the integration on and off times respectively, V_{GC} is the chromatograph signal voltage and V_{BC} is the baseline correction voltage. The integrator, at the end of each peak, prints out the count and the time of the peak. In these experiments the hydrogen peak is experienced at approximately 70 seconds after the beginning of the analysis. The integrator is connected to unused relay contacts in the auto sampler of the gas chromatograph so it will start when the gas chromatograph starts analyzing and resets after the gas chromatograph is finished (Figure 4). Control settings are the same for all runs as follows:

Recorder - 1
Peak sensitivity - 2
Power - on

3. Gamma Cell:

An Atomic Energy of Canada Limited, Model 220, Co^{60} well type gamma cell is used for the irradiation. The gamma cell has entry ways that allow gas flow via tygon tubing to the radiation vessel in the radiation well.

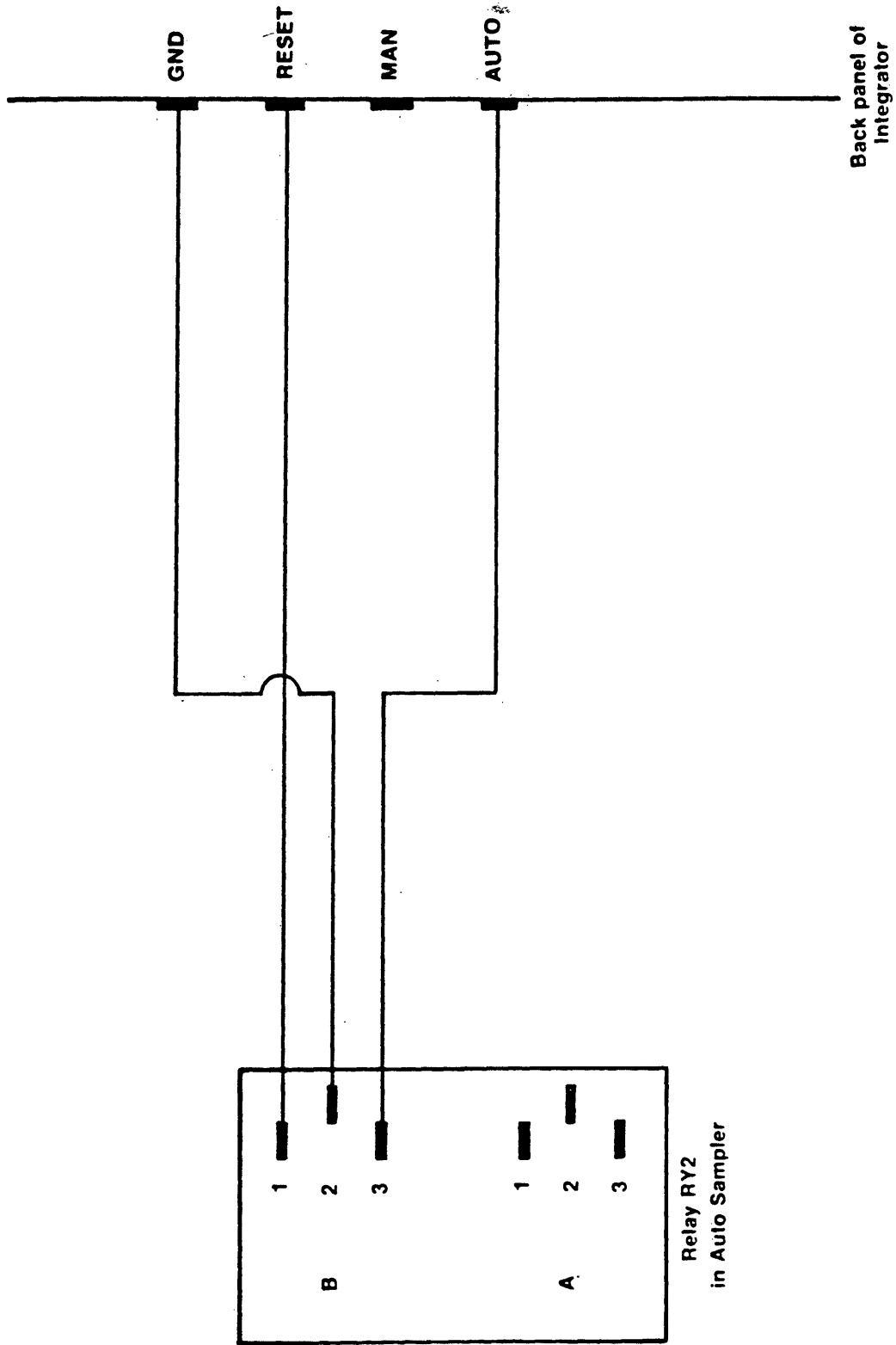


Figure 4 — Automation of Integrator

The cell is located at the Veterans Administration Hospital, Denver, Colorado. The measured dose rate was 3.4×10^5 rads/hr on September 29, 1977.

4. Flow Controller:

A Whitey micrometer valve #B-22R54 and Moore flow controller model SD63SUL are used to adjust and regulate the flow of the nitrogen transport gas. The flow controller is a differential type controller (see Figure 5). When the input pressure P_1 is applied to the valve and to the top of the controller's diaphragm, the diaphragm and plunger are forced down. The differential spring and downstream pressure P_2 force the diaphragm and plunger up. The differential spring produces an upward force equivalent to one produced by a constant pressure K . A pressure drop ΔP is developed across the micrometer valve due to its restriction of the flow. The controller is balanced when $P_1 = P_2 + K$, but $\Delta P = P_1 - P_2$, then $\Delta P = K$, thus the flow is constant.

5. Flowmeter:

Two Fisher Porter model #10A2735B ball type flowmeters are used to measure the flow rate of both nitrogen gas flows. The transport gas flow is normally set at 50cc/min and the gas chromatograph carrier gas flow at 10cc/min. It was found that the flowmeters were not linear and did not indicate actual flow rates. A correction factor for the readings is necessary to adjust the flow rates to actual cc/min. (See Calibration of Flow Meter).

6. Chart Recorder:

An Esterline Angus 0-10 millivolt strip chart recorder in conjunction with an Omega Omni -Amp ii millivolt amplifier is used to graph the

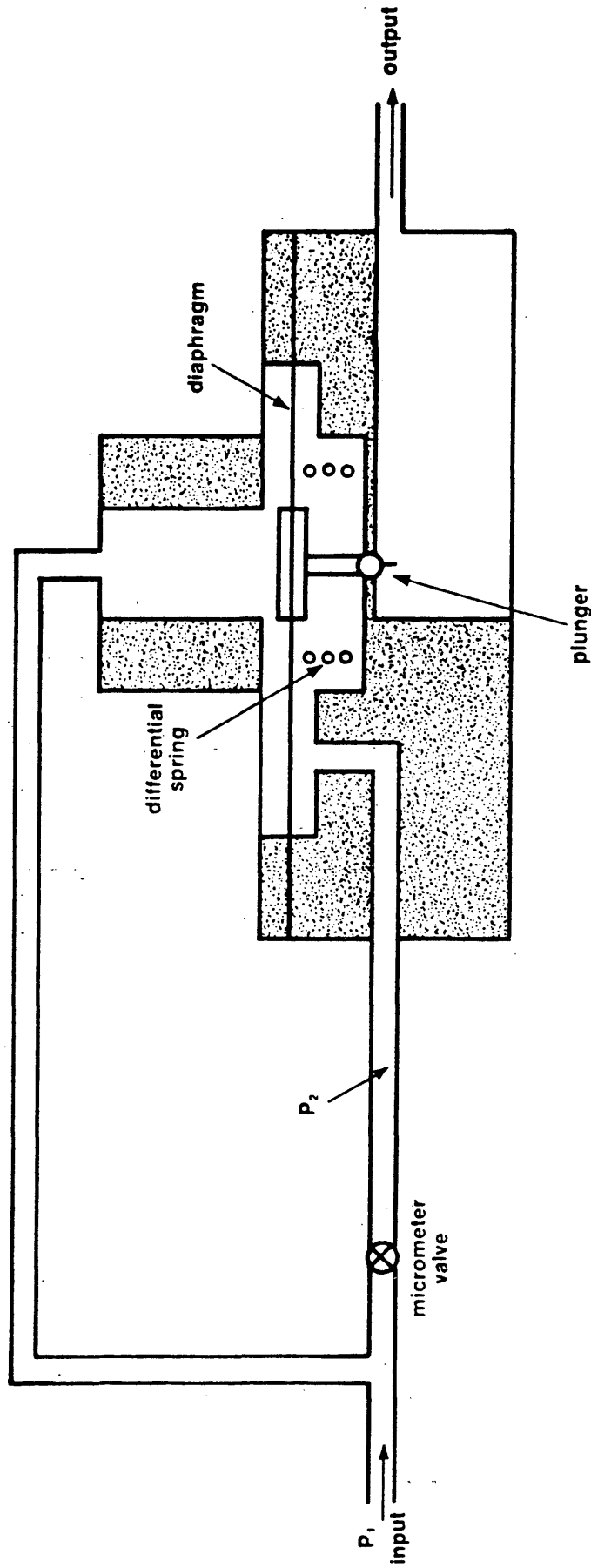


Figure 5 — Differential Flow Controller

output of the gas chromatograph. The recorder and amplifier are used to monitor the output during the setup and certain calibrations. A typical graph is shown in Figure 6. The recorder is run at a speed of .75 inches per minute and the amplifier gain at x5.

7. Radiation Vessel:

The radiation vessels used are made of pyrex glass by R. H. Allen Company, Boulder, Colorado. The vessels are cylindrical in shape 3.8cm O.D. and a height of 16.3cm (Figure 7). A medium size porous glass frit is located 1.5cm from the bottom of the vessel with an inlet tube for nitrogen gas located below the frit. A removable cap with a 1/4 inch glass tube for nitrogen exit, is used for access into the vessel (for filling, emptying and cleaning). A special aluminum holder was made to support the vessel in an upright position while in the gamma cell (Figure 8). The bottom of the vessel goes into the support and is held upright by three two inch long aluminum wires which are fastened to the base of the support. Nitrogen flows through the frit, bubbling through the water, suspending the powder catalyst and exiting through the cap transporting any gases produced by water decomposition.

8. Drierite Filter:

To maintain optimum performance of the gas chromatograph columns the transport gas must be free of moisture. A 2ft x 1 1/2 inch glass tube filled with indicating drierite #4 and #6 is used to dry the transport gas before entering the gas chromatograph. The glass tube is filled with drierite with the exception of approximately two inches at each end which is filled with glass wool and plugged with one hole rubber stoppers with short pieces of glass tubing extending

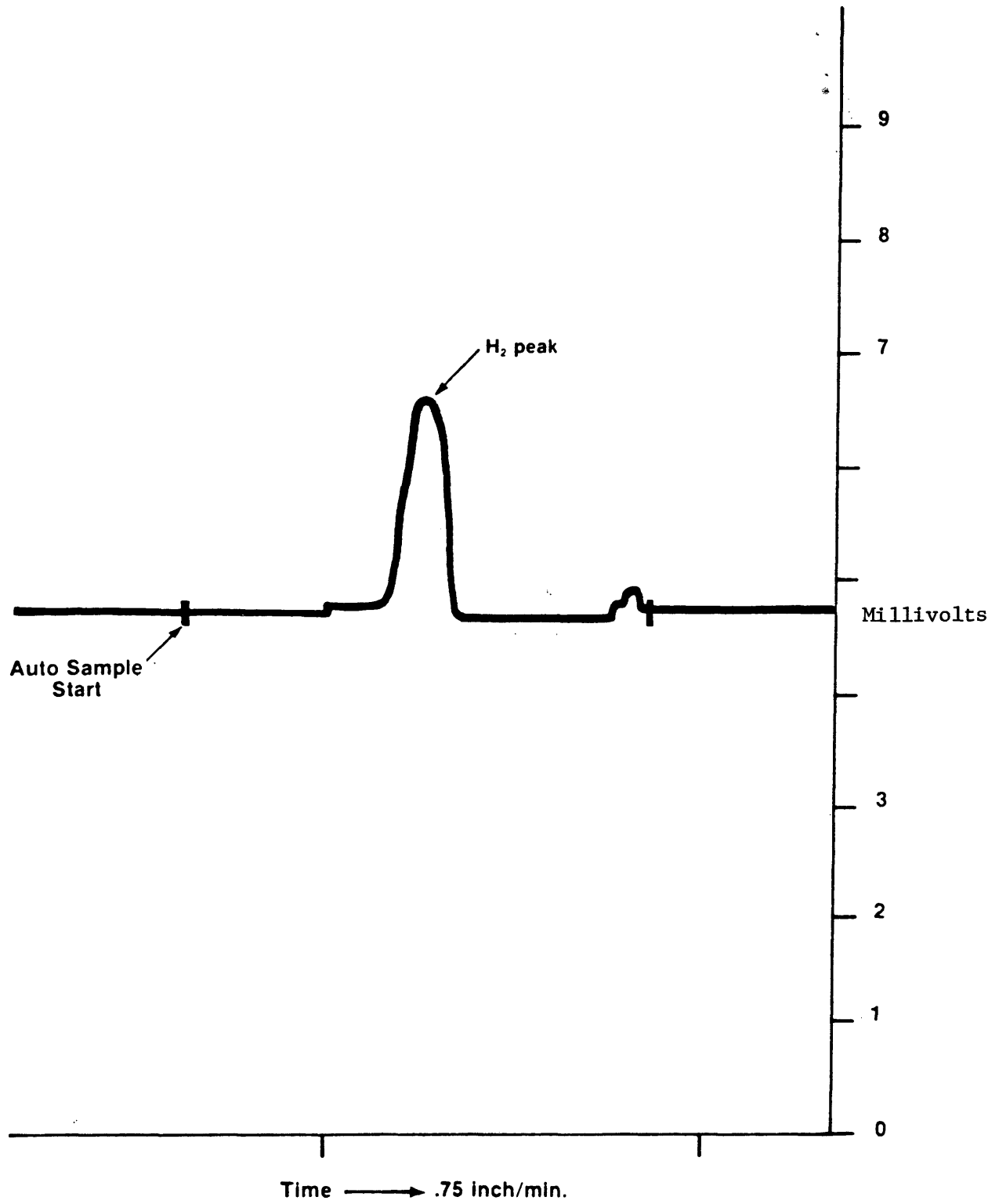


Figure 6 — Typical H₂ Peak

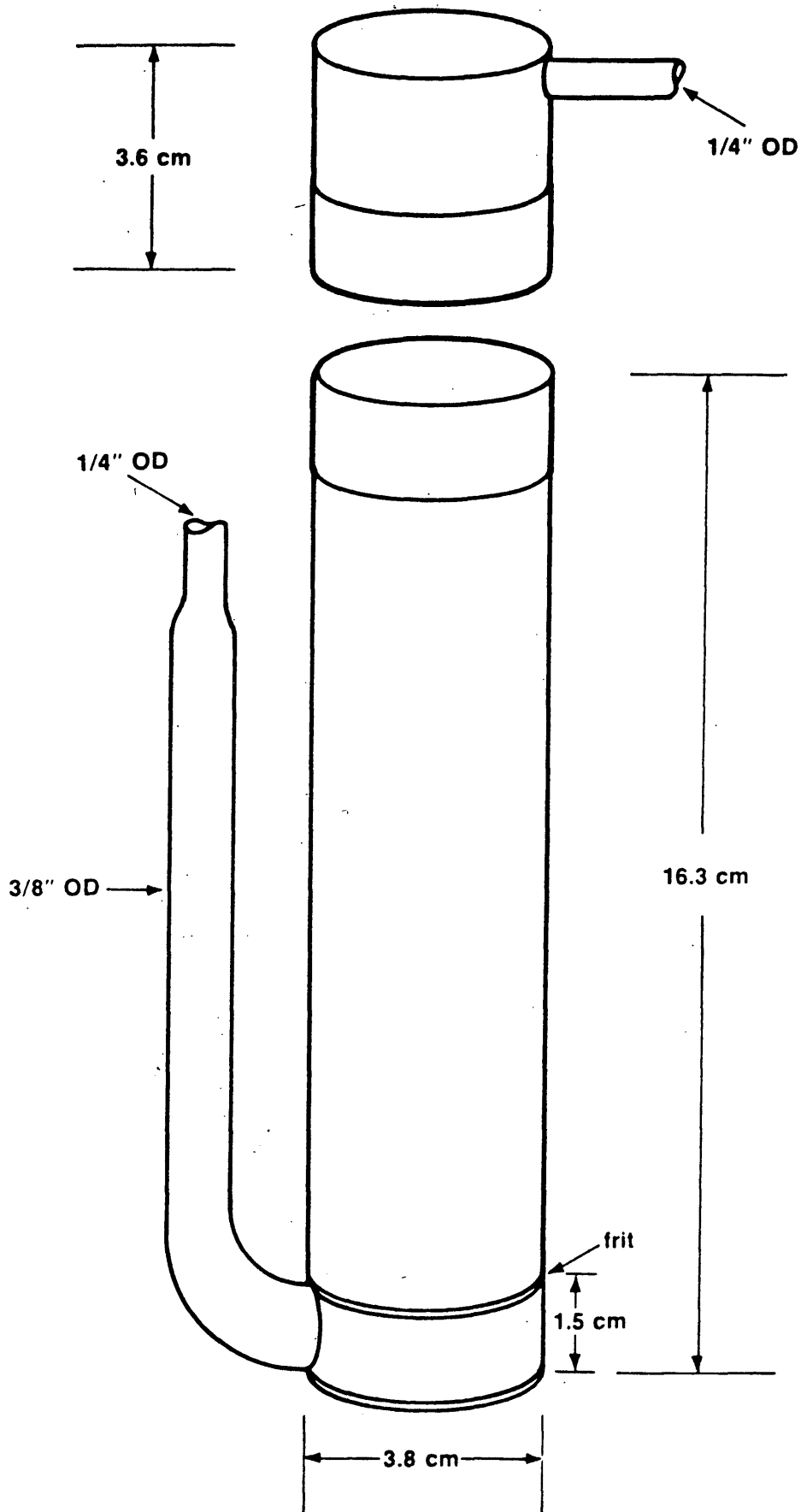


Figure 7 — Radiation Vessel

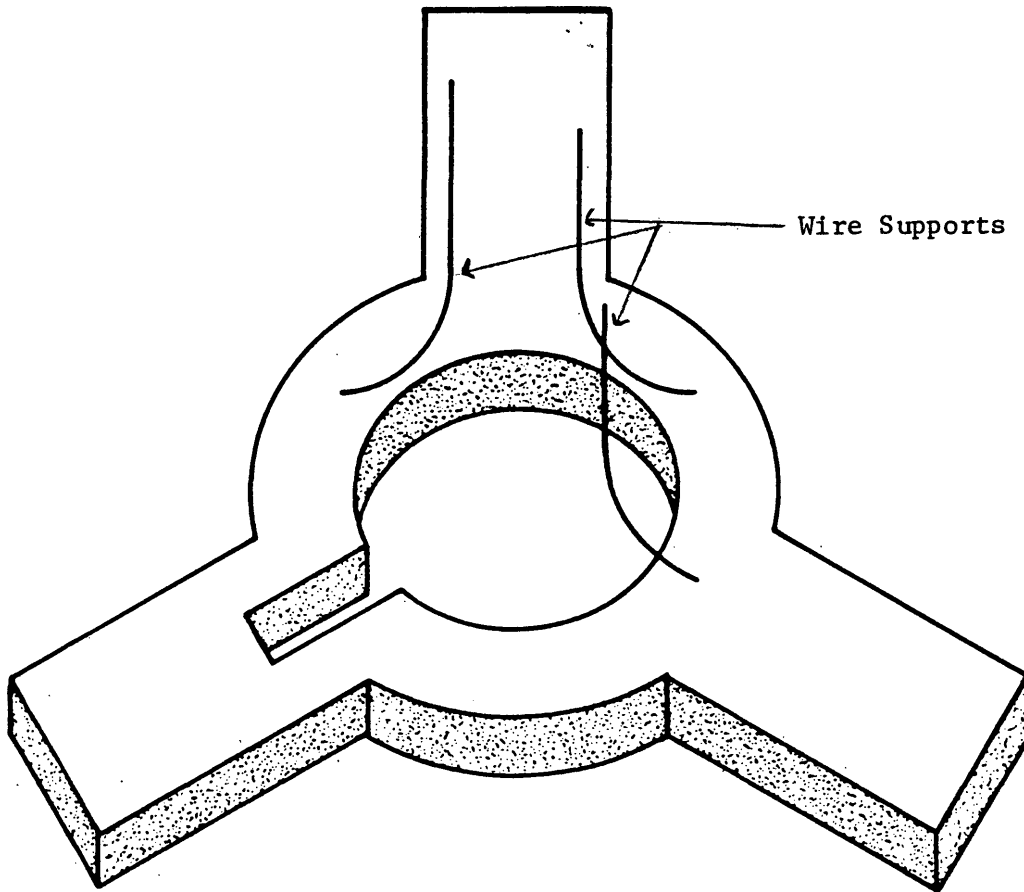


Figure 8 — Radiation Vessel Support

from the stoppers for entry and exit of the gas. The drierite turns from blue to pink upon absorbance of moisture. The filter needs to be changed only once in three months of nearly continuous use.

PROCEDURE

1. Integrator, recorder, and Omni-Amp are warmed up for a minimum of fifteen minutes with control settings as described in the experimental design section. Normally the gas chromatograph is left on continuously with the carrier gas flowing through it. If the gas chromatograph is shut down, it is necessary for it to warm up a minimum of one hour with control setting as described in the experimental design section. During this warm up period, nitrogen flows through the gas chromatograph sample loop and is sampled a minimum of every five minutes. This purges the gas chromatograph columns.
2. Radiation vessel is cleaned thoroughly with deionized water.
3. Radiation vessel is filled with 100cc deionized water and the lid is placed on the vessel.
4. The Gamma Cell well is raised and the vessel is placed in its support in the well. Tygon tubing, connected to the flow controller, going in to the Gamma Cell, via entry ports, is connected to the inlet tube of the vessel. Similarly, the tygon tubing going to the drierite filter is connected to the exit tube in the lid of the vessel.
5. The micrometer valve is opened approximately one quarter of maximum. Transport gas regulator pressure is increased until (usually 50-70 psi) a reading of 50cc/min is measured by the flowmeter.
6. The lid is removed from the radiation vessel and the catalyst (.75 grams) is poured in. The lid is then replaced.
7. The micrometer valve is adjusted as necessary to bring the flow rate to 50cc/min.

8. The system is allowed to stabilize for fifteen minutes. Any impurities in the system normally are swept out by the transport gas in this time. The gas chromatograph sampler is activated. If any impurities are detected by the gas chromatograph, samples are taken every five minutes until the system becomes clean.

9. The flow rate is checked and adjusted, if necessary, to 50cc/min. The auto sampler is set for desired sample frequency, usually 30 minute intervals. The well of the Gamma Cell is closed and lowered into the radiation field. Simultaneously the auto sampler is activated so that the beginning of the first sample coincides with the beginning time of the sample being irradiated.

10. The system is normally run for 24 hours.

11. After the run is completed:

- Raise Gamma Cell well.
- Turn off transport gas.
- Disconnect tygon tubes from vessel.
- Remove vessel from well.
- Turn auto sampler off.

12. If another run is to be initiated the above procedure is repeated. If another run is not to be initiated then:

- Integrator, Omni-Amp, and recorder are turned off.
- Gamma Cell well is lowered into cell.

FLUX MEASUREMENT OF THE GAMMA CELL

The Fricke dosimetry method (7) was used to determine the radiation flux of the gamma cell at the Veterans Administration Hospital, located in Denver, Colorado on September 29, 1977. This method is based on the radiation induced oxidation of ferrous ion to ferric ion. The extent of oxidation is related quantitatively to the gamma energy deposited in the water solution.

The preparation of the chemical solution is as follows:

1. A 250 ml solution of 0.40M H_2SO_4 is prepared.
2. Added to this solution is 0.001 M NaCl.
3. Oxygen is then bubbled through the solution for ten minutes.
4. Five grams of $Fe(NH_4)_2(SO_4)_2 \cdot 6H_2O$ (ferrous ammonium sulfate) is then dissolved in the solution.

The solution was transported to the gamma cell at the Veterans Administration Hospital. Eight labeled sealed glass vials were filled with 15 ml each of the ferrous solution. Two vials were placed in the gamma cell and exposed to the radiation for two minutes. The vials were then removed and replaced with two unirradiated vials. These vials were exposed to the radiation for four minutes. The above procedure was repeated with unirradiated vials for six and eight minutes.

The eight vials were analyzed to determine the absorbance values of ferric ions relative to an unirradiated sample of the solution. The absorbance was measured with a Beckman DU II spectrophotometer using standard 1cm silica cells at 304 m μ . At this wavelength the

ferrous ions have negligible absorbance. The absorbance values for the samples are listed in Table 2.

The absorbed dose D(rads) is calculated by the following formula for a 0.40M H₂SO₄, 1 cm absorption cells and G(Fe³⁺)=15.6 (7).

$$D=2.75 \times 10^4 \times \Delta A \quad (3)$$

Where ΔA is the relative absorbance. The optical density measurements are performed at 25°C. A temperature correction factor of 0.69% per degree is used (7). Then:

$$D(\text{rads})=(2.75 \times 10^4)(\Delta A)(1 + .0069(T-25)) \quad (4)$$

Table three lists the results obtained using equation (4).

The attenuation due to the glass vial was also considered.

$$I=I_0 e^{-ux} \quad (5)$$

I_0 =unattenuated dose rate.

I =attenuated dose rate= 5.67×10^3 rads/min.

u =Glass linear absorption coefficient for gamma rays of 1.5 Mev= $.14 \text{ cm}^{-1}$.

x =thickness of attenuater = .15 cm.

The unattenuated dose rate $I_0=5.79 \times 10^3$ rads/min.

The attenuation due to the glass radiation vessels used in the experiments was also taken in consideration. Using equation (5), with $x=.23 \text{ cm}$, the dose rate in the radiation vessel was found to be 5.61×10^3 rads/min.

Since Co⁶⁰ has a half life of 5.3 years, it is necessary to correct the dose rate with time using equation (6). The results can be found in Table 3.

$$I=I_0 e^{-\lambda t} \quad (6)$$

where λ =disintegration constant for Co⁶⁰ is equal to $.13 \text{ yr}^{-1}$

t =time elapsed in years.

<u>Sample</u>	<u>Exposure time (sec.)</u>	<u>Absorbance (A)</u>	<u>Temperature=26°C</u>
* 1	120	0.082	
* 2	120	0.175	
3	240	0.808	
4	240	0.820	
5	360	1.230	
6	360	1.230	
7	480	1.650	
8	480	1.650	
* 1	120	0.100	
* 2	120	0.186	

* Samples #1 and #2 were reanalyzed but were not used in the calculation of the dose rate because of their inconsistent absorbance values.

Table 2. Absorbance Values.

<u>Sample</u>	<u>Exposure time (min.)</u>	<u>D (rads)</u>	<u>D (Rads/min.)</u>
3	4	2.24×10^4	5.59×10^3
4	4	2.27×10^4	5.68×10^3
5	6	3.41×10^4	5.68×10^3
6	6	3.41×10^4	5.68×10^3
7	8	4.57×10^4	5.71×10^3
8	8	4.57×10^4	5.71×10^3

$$\bar{D} = 5.67^{+0.04} \times 10^3 \text{ rads/min}$$

Table 3. Dose Rate Values.

<u>Time (months)</u>	<u>Attenuated Radiation Dose (rads/min)</u>	<u>Percent of Initial Dose Rate</u>
0	5.67×10^3	—
1	5.61×10^3	98.9
2	5.51×10^3	97.2
3	5.48×10^3	96.6
4	5.43×10^3	95.8
5	5.38×10^3	94.9
6	5.32×10^3	93.8
7	5.26×10^3	92.8
8	5.20×10^3	91.7
9	5.15×10^3	90.3
10	5.09×10^3	89.8
11	5.04×10^3	88.9
12	4.98×10^3	87.8

Table 4. Change in Radiation Dose with Time.

CALIBRATION OF GAS CHROMATOGRAPH AND INTEGRATOR

Two calibration gases were obtained from Union Carbide, Los Angeles, California. Calibration gas #1 was a 45.7[±]3%ppm mixture of molecular hydrogen in nitrogen. Calibration gas #2 was a 481[±]3%ppm mixture of molecular hydrogen in nitrogen. Certification of analysis was made by the vendor. Several runs of these gases were made in order to calibrate the output of the gas chromatograph and integrator. The results of these runs are shown in Table 5.

Since the gas chromatograph measures the actual number of molecules and not ppm directly, an error in the number of H₂ molecules per unit volume is introduced due to variations in temperature and pressure. United States Weather Bureau statistics indicate that maximum and minimum pressure in the Denver area for the last year was 63.88 and 60.96 cm of Hg respectively. Using the pressure as 62.42 cm of Hg [±]1.46 and the temperature as 40.0[°]C [±].001[°]C and using the ideal gas law, the total number of molecules per cubic centimeter (n/v) is 1.92x10¹⁹ [±] .05x10¹⁹. To convert counts (C) from the integrator to actual number of hydrogen molecules per cubic centimeter (n_H), the following equation is used.

$$n_H = \left(\frac{n}{v}\right) C / K \times 10^6 \left(\frac{1}{2}\right) = 9.60 \times 10^{12} \left(\frac{C}{K}\right) \quad \text{where } K = C/\text{ppm} \quad (7)$$

The factor of 1/2 is introduced because the gas chromatograph analyzes a 2 ml sample.

Table 5. Results of Calibration Gas Runs

Calibration Gas H ₂ in N ₂ (ppm)	Run #	# of Samples	\bar{C} Mean Value of Counts	ΔC	K Counts/ppm K=C /ppm	ΔK^*
45.7 \pm 3%	102	45	770	110	16.9	2.5
45.7 \pm 3%	103	41	880	110	19.3	2.5
45.7 \pm 3%	112	25	800	110	17.5	2.5
481 \pm 3%	114	38	9280	130	19.3	0.6

$$*\Delta K = \left[\left(\frac{\partial K}{\partial C} \right)^2 (\Delta C)^2 + \left(\frac{\partial K}{\partial \text{ppm}} \right)^2 (\Delta \text{ppm})^2 \right]^{\frac{1}{2}}$$

CALIBRATION OF FLOW METER

A soap bubble meter is used for calibration of the flow meter. The bubble meter is made from a 250 ml graduated burette with a rubber bulb on the bottom and a gas inlet fitting above the bulb on the side. (See Figure 9). The gas enters the bubble meter, and when the bulb is squeezed, a soap bubble is formed and travels up the tube at the gas flow rate. A stop watch was used to time the travel of the bubble. By knowing the time and the volume displaced during the bubble's travel, the flow rate can be calculated by the following equations (See Table 6 and Figure 10).

$$8) \quad \bar{F}_{RA} = 60 \bar{V}_D / \bar{T} \text{ (cc/min)}$$

$$9) \quad \Delta T = \left[\sum (T_i - \bar{T})^2 / (n-1) \right]^{1/2}$$

$$10) \quad \Delta F_{RA} = \left[\left(\partial F_{RA} / \partial V \right)^2 (\Delta V)^2 + \left(\partial F_{RA} / \partial T \right)^2 (\Delta T)^2 \right]^{1/2}$$

V_D = Volume displaced by soap bubble measures in cc.

T = Time for bubble to displace volume V_D in seconds.

F_{RA} = Actual flow rate of gas measured in cc/min.

F_{RM} = Reading of flow meter in cc/min.

n = Number of measurements.

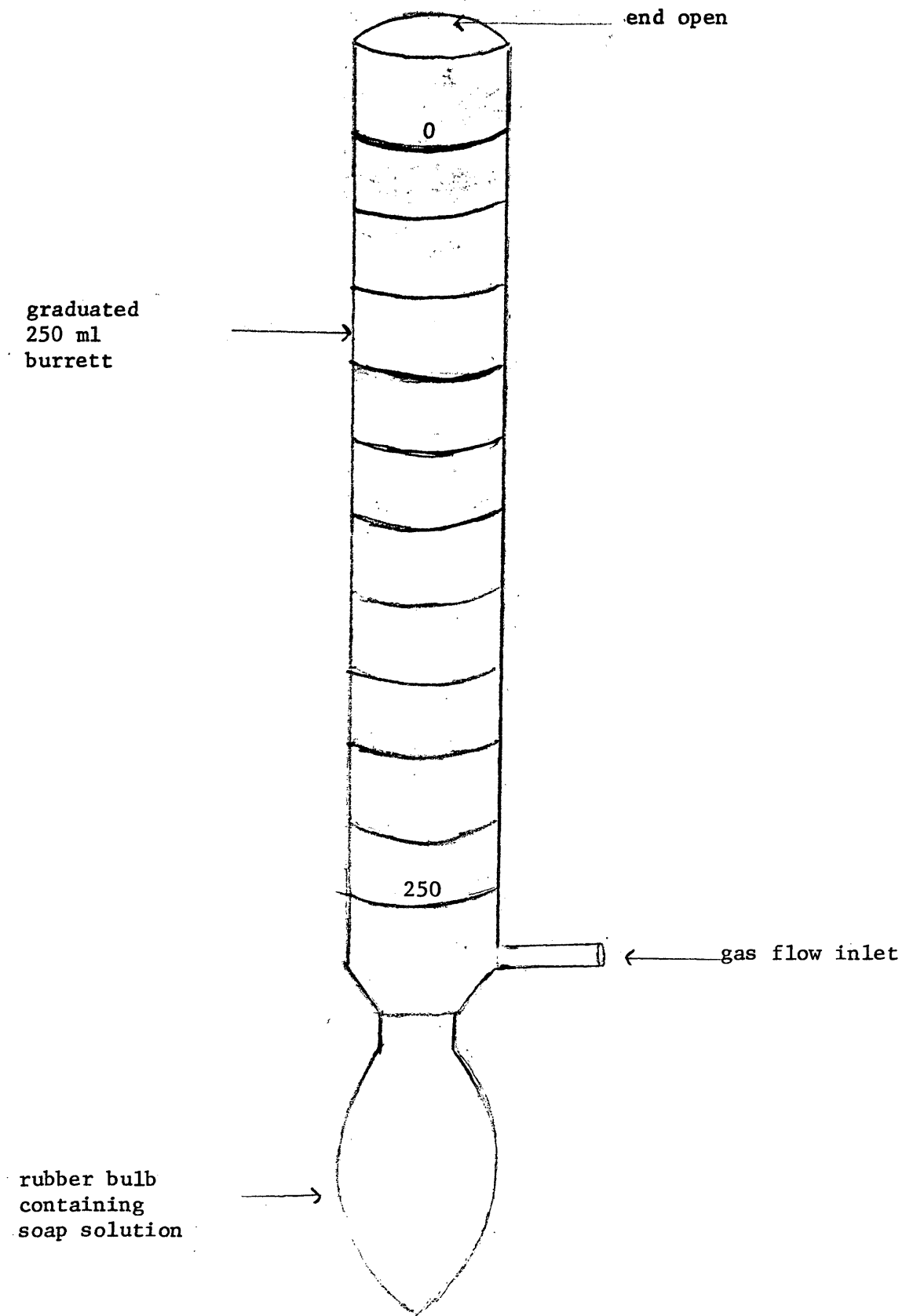


Figure 9 Soap Bubble Meter

Table 6. Calibration of Flow Meter

n	\bar{V}_D	\bar{T}	ΔT	V_D	\bar{F}_{RA}	ΔF_{RA}	F_{RM}
5	50.0	35.2	0.2	0.5	85.2	.98	83
5	50.0	39.4	0.1	0.5	76.1	.79	75
5	40.0	40.8	0.1	0.5	58.8	.75	60
5	30.0	34.4	0.2	0.5	52.4	.92	55
5	30.9	38.9	0.3	0.5	46.3	.86	50
5	30.0	40.6	0.5	0.5	44.3	.92	48
5	30.0	43.4	0.2	0.5	41.5	.72	45
5	30.0	49.4	0.4	0.5	36.4	.70	40
5	30.0	84.0	0.2	9.5	21.2	.36	25
5	30.0	90.8	0.3	0.5	19.8	.34	23
5	20.0	73.4	1.4	0.5	16.4	.51	20

V_D = Volume displaced by soap bubble measured in cc.

T = Time for bubble to displace volume V in seconds

F_{RA} = Actual flow rate of gas measured in cc/min.

F_{RM} = Reading of flow meter in cc/min.

n = number of measurements

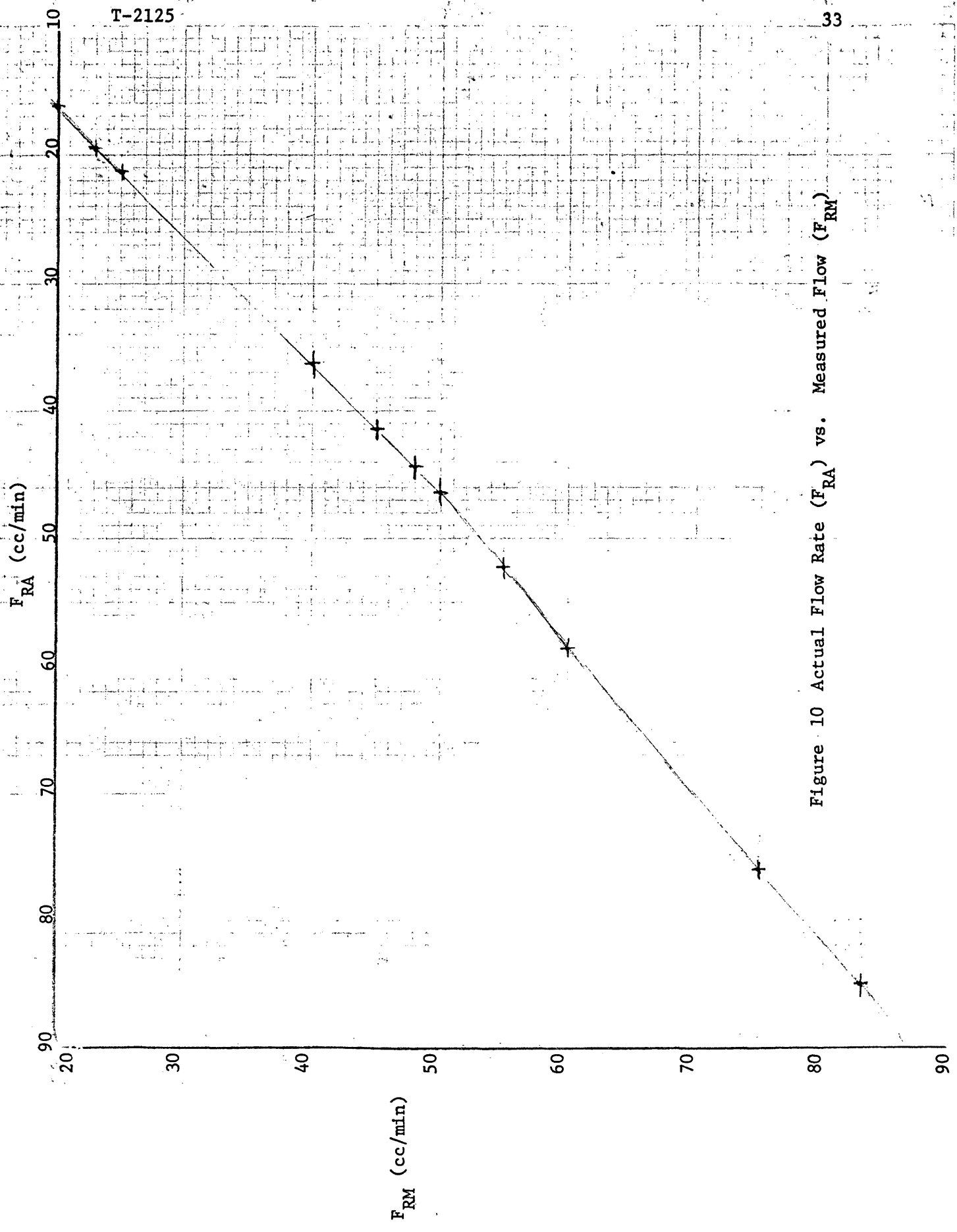


Figure 10 Actual Flow Rate (F_{RA}) vs. Measured Flow (F_{RM})

EXPERIMENTAL RESULTS

Eight different solids (See Table 7) were tested for performance as catalysts in individual experiments. All experiments were performed with 100 cc H₂O and .75 grams of the catalyst with the exception of run #137 where .25 grams of MgO is used (.75 grams of MgO clogs the frit). Most runs are for 24 hours with automatic sampling at 30 minute intervals. The results of these runs are graphed and are shown in Appendix I. The graphs plot integrator count (C) versus time in the gamma radiation field for a corrected actual nitrogen transport flow rate of 46.3cc/min. (50cc/min. flow rate indicated by the flow meter is actually 46.3cc/min. See Calibration of Flowmeter). The integrater count (C) is a measure of the amount of molecular hydrogen produced. Figures 24-26 (Appendix I) represent runs with 100cc H₂O in the absence of solids. The latter were used for baseline data, as they indicate quantities of molecular hydrogen generated from the interaction of only the gamma radiation with water.

A 300 minute time interval is selected for analysis from each run. This selection is based on maximum average hydrogen detection. The intervals selected are indicated by arrows on the Figures 13-26 in Appendix I. The integrator counts are averaged for each run in the 300 minute interval (See Table 7). Average values (\bar{C}_A) for different runs but using the same catalyst are also averaged and the results are shown in Table 8. The uncertainties ΔC_A in the integrator count were obtained from the calibrations of the gas chromatograph and integrator, except for the baseline data, where the standard deviation was used for the uncertainty. A plot of average count, \bar{C}_A , versus band gap is shown in Figure 11.

SnO_2 (Eg=4.3 ev) exhibits the greatest molecular hydrogen yield ($C_A = 6660$) relative to the other powders tested. Baseline average count was 4870. Solids tested with band gaps lesser or greater than SnO_2 indicate a lower hydrogen yield relative to SnO_2 .

The integrator counts can be converted to parts per million (ppm) of Hydrogen (Table 8).

$$11) \quad \text{where ppm} = \bar{C}_A / K \quad K = 19.3 \pm 0.6 \quad (\text{See Calibration of Gas Chromatograph and Integrator})$$

$$12) \quad \text{and } \Delta \text{ppm} = \left[\left(\frac{\Delta C_A}{K} \right)^2 + \left(\frac{C_A}{K} \right)^2 (\Delta K)^2 \right]^{1/2}$$

$G_{(\text{H}_2)}$ values are also obtained. ($G_{(\text{H}_2)}$ is the amount of H_2 molecules formed per 100 ev. deposited in the water.) (7)

$$13) \quad G_{\text{H}_2} = 100 \frac{n_{\text{H}} F_{\text{RA}}}{D}$$

$$14) \quad \text{and } \Delta G_{\text{H}_2} = 100 \left[\left(\frac{F_{\text{RA}}}{D} \right)^2 (\Delta n_{\text{H}})^2 + \left(\frac{n_{\text{H}}}{D} \right)^2 (\Delta F_{\text{RA}})^2 + \frac{(n_{\text{H}} F_{\text{RA}})^2}{D^2} (\Delta D)^2 \right]^{1/2}$$

$$15) \quad n_{\text{H}} = \left(\frac{n}{V} \right) (\bar{C}_A / K) 1/2 \times 10^6 = \left(\frac{n}{V} \right) (\text{ppm}) 1/2 \times 10^6$$

where $\left(\frac{n}{V} \right) = 1.92 \times 10^{19} \pm 0.05 \times 10^{19}$ molecules/cc

$$16) \quad \Delta n_{\text{H}} = 1/2 \times 10^6 \left[(\text{ppm})^2 \left(\frac{\Delta n}{V} \right)^2 + \left(\frac{n}{V} \right)^2 (\Delta \text{ppm})^2 \right]^{1/2}$$

where n_{H} = number of H_2 molecules/cc

F_{RA} = actual flow rate = 46.3 ± 0.9 cc/min

D = dose rate = 5.20×10^3 rads/min

= $3.25 \times 10^{19} \pm 0.03 \times 10^{19}$ ev/(100gm)(min) for H_2O

These values are shown in Table 8.

Table 7 - Radiation Catalysis Tests

<u>Run Number</u>	<u>Catalyst</u>	<u>Grams</u>	<u>(cc)</u> <u>H₂O</u>	<u>Number of</u> <u>Points</u>	<u>C_A*</u> <u>Average Counts</u>
118	---	---	100	10	4910
132	---	---	100	10	4710
139	---	---	100	10	5010
121	MoO ₃	.75	100	10	4590
127	MoO ₃	.75	100	10	4620
134	In ₂ O ₃	.75	100	10	4740
120	TiO ₂	.75	100	14	5090
138	TiO ₂	.75	100	10	5070
128	V ₂ O ₅	.75	100	10	5340
119	MgO	.75	100	10	5580
137	MgO	.25	100	10	5820
136	Sb ₂ O ₃	.75	100	10	5850
131	HfO ₂	.75	100	10	6220
130	SnO ₂	.75	100	10	6660

*C_A = average counts for 300 minutes

Table 8. Values for n_H , ppm, G_{H_2} , for the Catalysts

Catalyst	Count \bar{C}_A	ΔC_A	n_H ($\times 10^{15}$)	Δn_H ($\times 10^{15}$)	ppm \bar{C}_A/K	Δppm	$G_{(H_2)}$	ΔG_{H_2}	Band Gap* ev
Baseline	4870	150	2.4	0.1	252	11	0.35	0.02	---
MoO ₃	4610	130	2.3	0.1	238	10	0.29	0.02	2.8
In ₂ O ₃	4740	130	2.4	0.0	245	10	0.34	0.02	2.619
TiO ₂	5080	130	2.5	0.1	263	10	0.36	0.02	3.0
V ₂ O ₅	5340	130	2.7	0.1	276	10	0.38	0.02	2.34
MgO	5700	130	2.8	0.1	295	11	0.40	0.02	7.77
Sb ₂ O ₃	5850	130	2.9	0.1	303	11	0.42	0.02	3.31
HfO ₂	6220	130	3.1	0.1	322	12	0.44	0.02	5.55
SnO ₂	6660	130	3.3	0.2	345	12	0.47	0.02	4.3

*"Compilation of Energy Band Gaps in Elemental and Binary Compound Semiconductors and Insulators", 1973 00. 163-199.

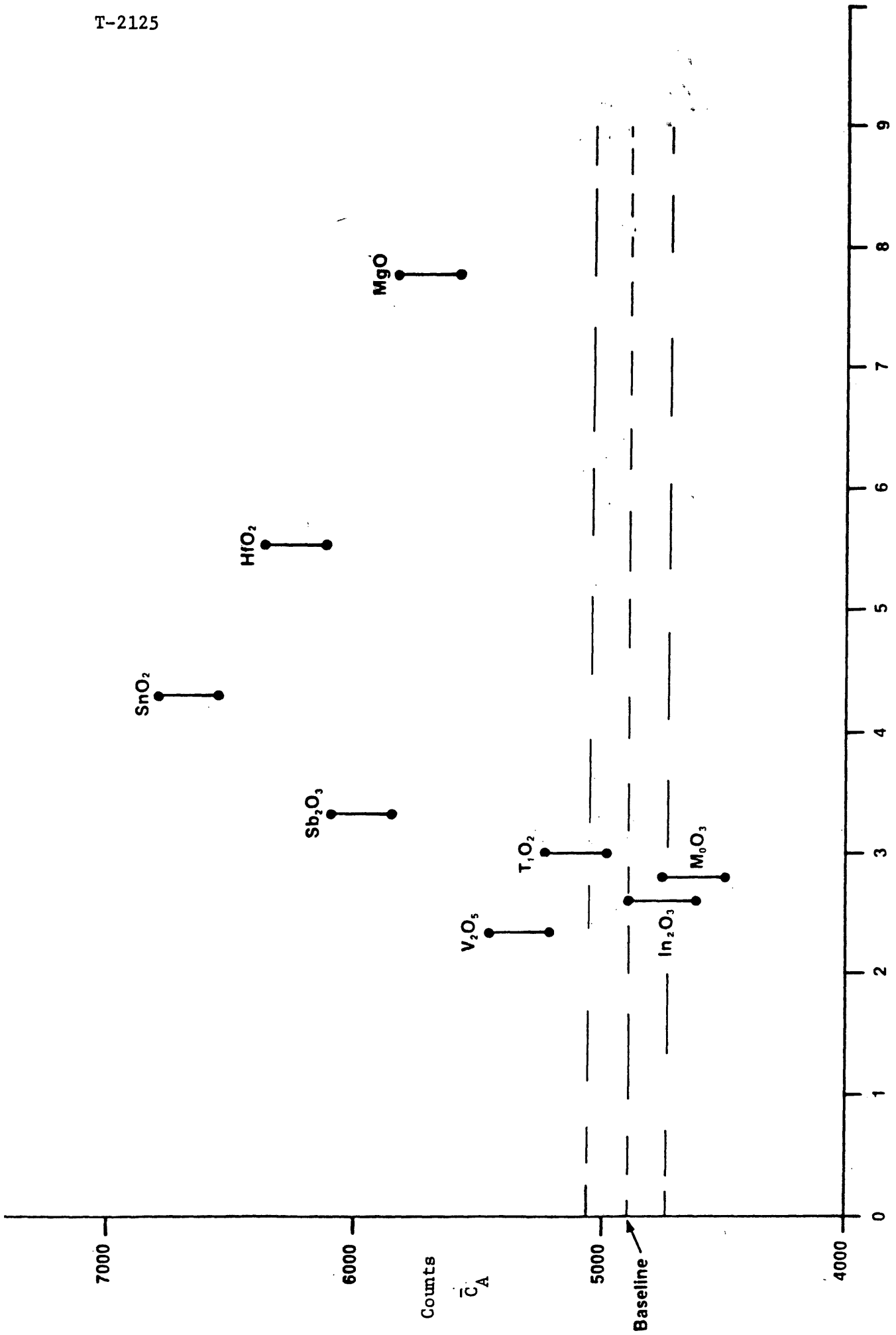


Figure 11 Band Gap of Catalyst vs. Average Integrator Counts

DISCUSSION OF RESULTS

SnO_2 (band gap (E_g)=4.3 ev) exhibits the greatest molecular hydrogen yield of the eight solid powders tested. Figure 11 indicates the maximum hydrogen yield occurs when the band gap of the solid is between 3.31 ev and 5.55 ev. This is consistent with the 4.79 ev bond energy of the water molecule.

The water molecules are being adsorbed on the surface of the powder catalyst and an increase in surface area of the powder may have an effect on catalytic activity (hydrogen yield). The particle sizes of the powders were not known, therefore the surface area cannot be directly correlated in the analysis of their catalytic activity. However, run #119 used 0.75 grams of MgO and the hydrogen yield was measured before the frit clogged. Run #137 used 0.25 grams of MgO and the difference in hydrogen yield of the two runs are within experimental error. This would indicate an increase of surface area of the solid catalyst above a minimum threshold value does not increase its catalytic activity.

All catalyst runs (except run #137 MgO) were made using 0.75 grams of solid powder catalysts. Different hydrogen yields were obtained using different catalysts, but the mass of the catalysts remained constant. Thus the difference in hydrogen yields cannot be attributed to differences in the mass. Also there is no correlation between catalytic activity and the density of the solid used.

The 300 minute time interval selected for analysis differed for each run. The interval selected for each run was based on maximum average hydrogen detection. Average maxima occurring at different

300 minute intervals for the runs can be attributed to a possible time dependence for catalytic activity or a difference in time necessary to reach thermal equilibrium in a radiation environment.

From the baseline data, $G(H_2)$ was found to have a value of 0.35. This differs from the expected experimental value of 0.45. The difference is most likely due to impurities in the water. The impurities combine with some of the hydrogen molecules produced by water decomposition. This restricts the amount of molecular hydrogen that can leave the radiation vessel. Therefore less molecular hydrogen is detected by the gas chromatograph and a lower $G(H_2)$ value is obtained.

CONCLUSION AND RECOMMENDATIONS FOR FUTURE WORK

A change in hydrogen production (or water decomposition) is found to be related to the band gap of the semiconductor or insulator catalyst (See Figure 12). The graph indicates an increase in water decomposition over baseline values when the band gap of the catalyst is greater than 3.0 electron volts. A maximum yield of the amount of hydrogen produced appears to occur when the band gap of the catalyst is greater than 3.31 electron volts and less than 5.55 electron volts. Water decomposition (catalytic activity) decreases and may approach baseline values when the band gap is greater than 5.55 electron volts. Catalysts with band gaps between 2.6 and 3.0 electron volts appear to have no effect on water decomposition. The amounts of hydrogen measured for these catalysts are within experimental error of baseline data.

Hydrogen yield using SnO_2 (band gap 4.3 eV) is 345 ppm compared with baseline values of 252 ppm. This catalyst gives the greatest yield of hydrogen, 37% increase over baseline values, in these experiments. This indicates the maximum hydrogen yield appears to occur with a catalyst with a band gap energy between 3.31 and 5.55 electron volts. The occurrence of a maximum between catalyst band gap energies of 3.31 and 5.55 electron volts brackets the bond energy of the water molecules which is equal to 4.79 eV/molecule.

Recommendations for future work would be to find where the maximum hydrogen yield occurs. Candidate catalysts would include BaO (band gap = 5.13 eV), MnO (band gap = 3.7 eV) and ZnO (band gap = 3.35 eV). (6)

Recommended research would be to study catalysts with band gaps greater than 7.7 electron volts, to see if the hydrogen yield does in fact approach baseline. Candidate catalysts would include BeO (band gap = 14.5 eV), Al₂O₃ (band gap = 9.9 eV) and SiO₂ (band gap = 8.4 eV).

Also recommended would be a more complete study of surface area effects in radiation induced heterogeneous catalytic reactions. A possible study might be made to see if chemical bonding in reactions occurring on the surface of solids can be correlated with the molecular hydrogen yield.

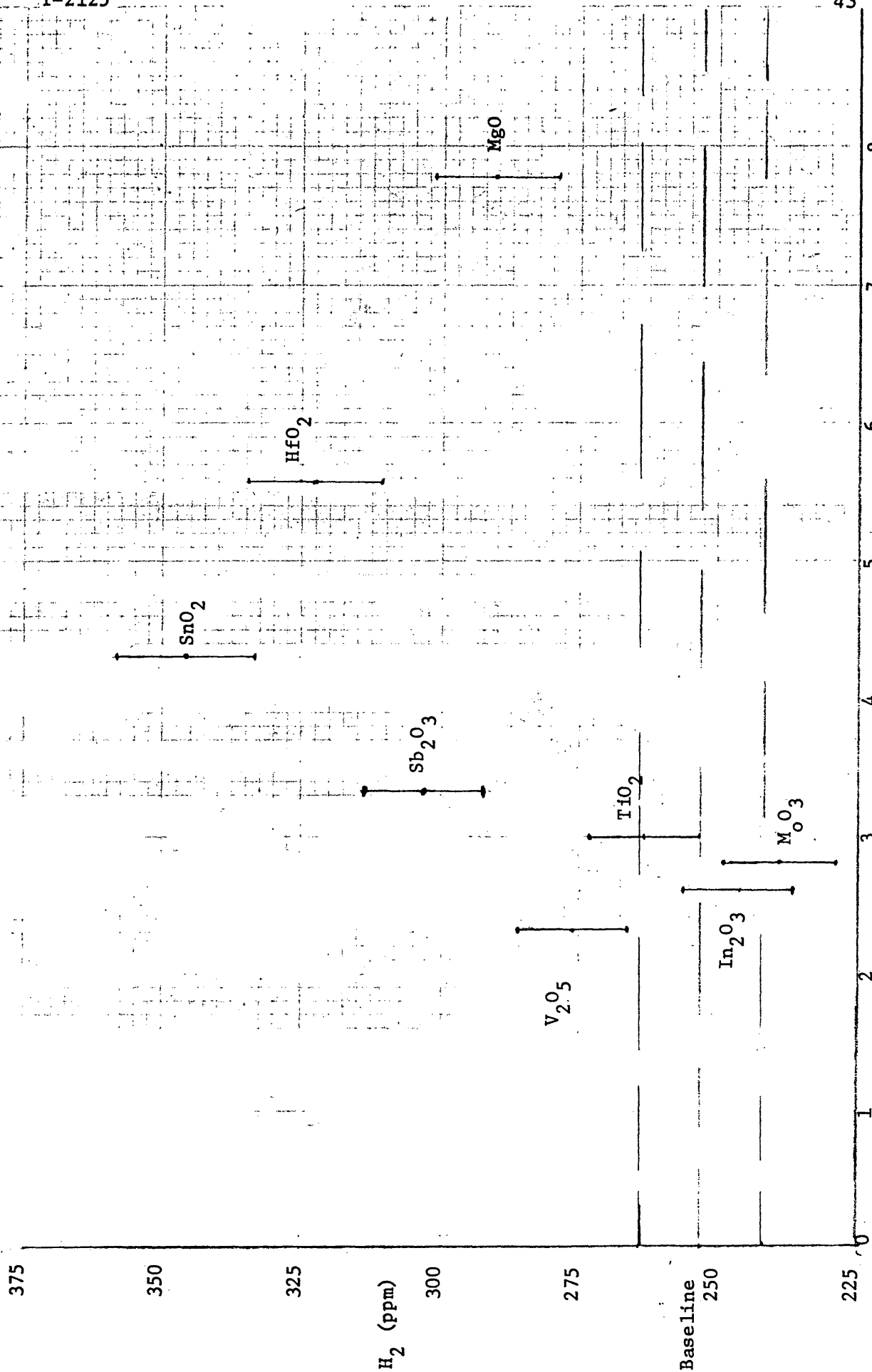


Figure 12 Band Gap vs. H₂ Yield (ppm)

APPENDIX I

GRAPHS OF EXPERIMENTAL DATA

T-2125

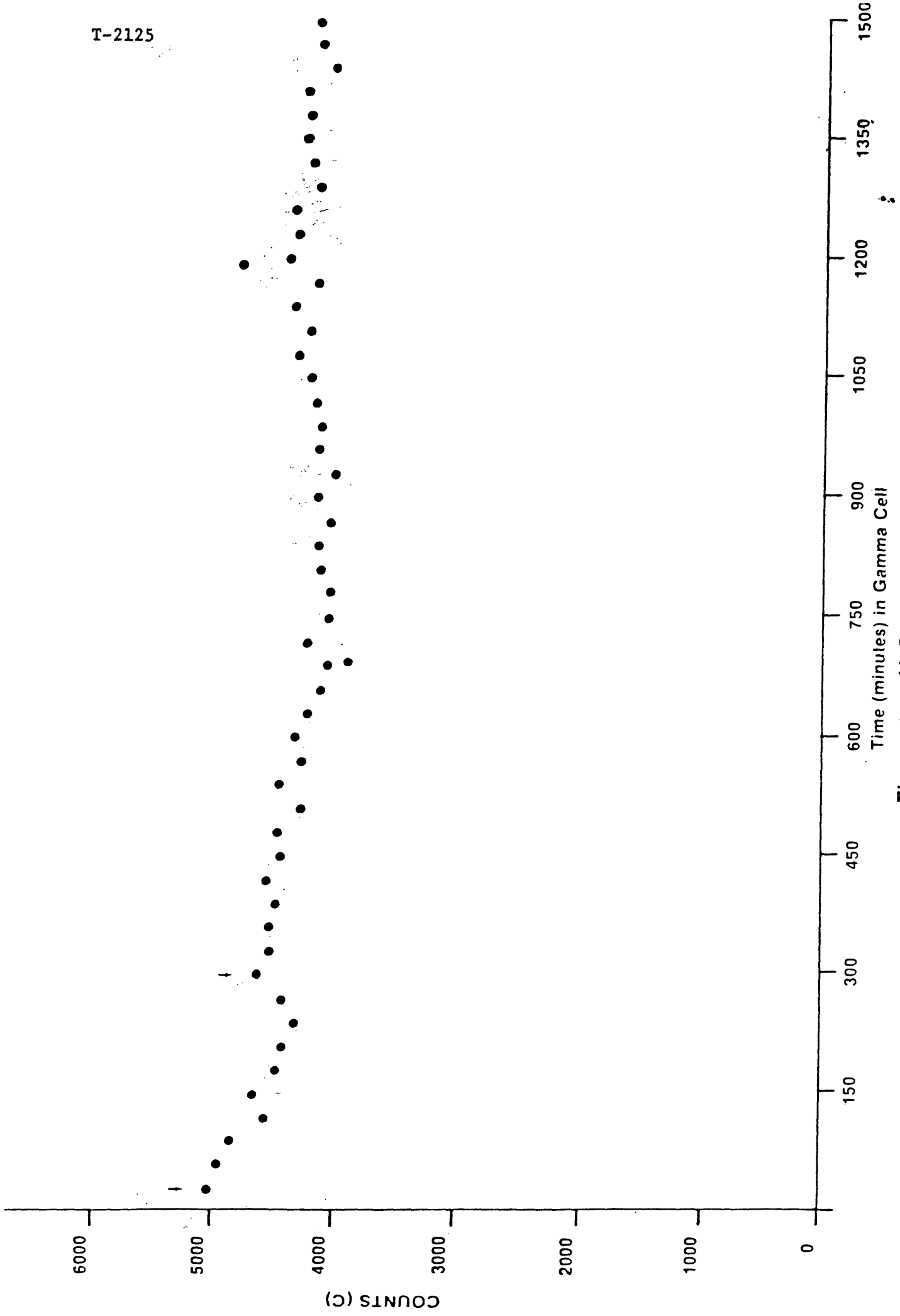


Figure13 — H₂O + M₀O (run #127)

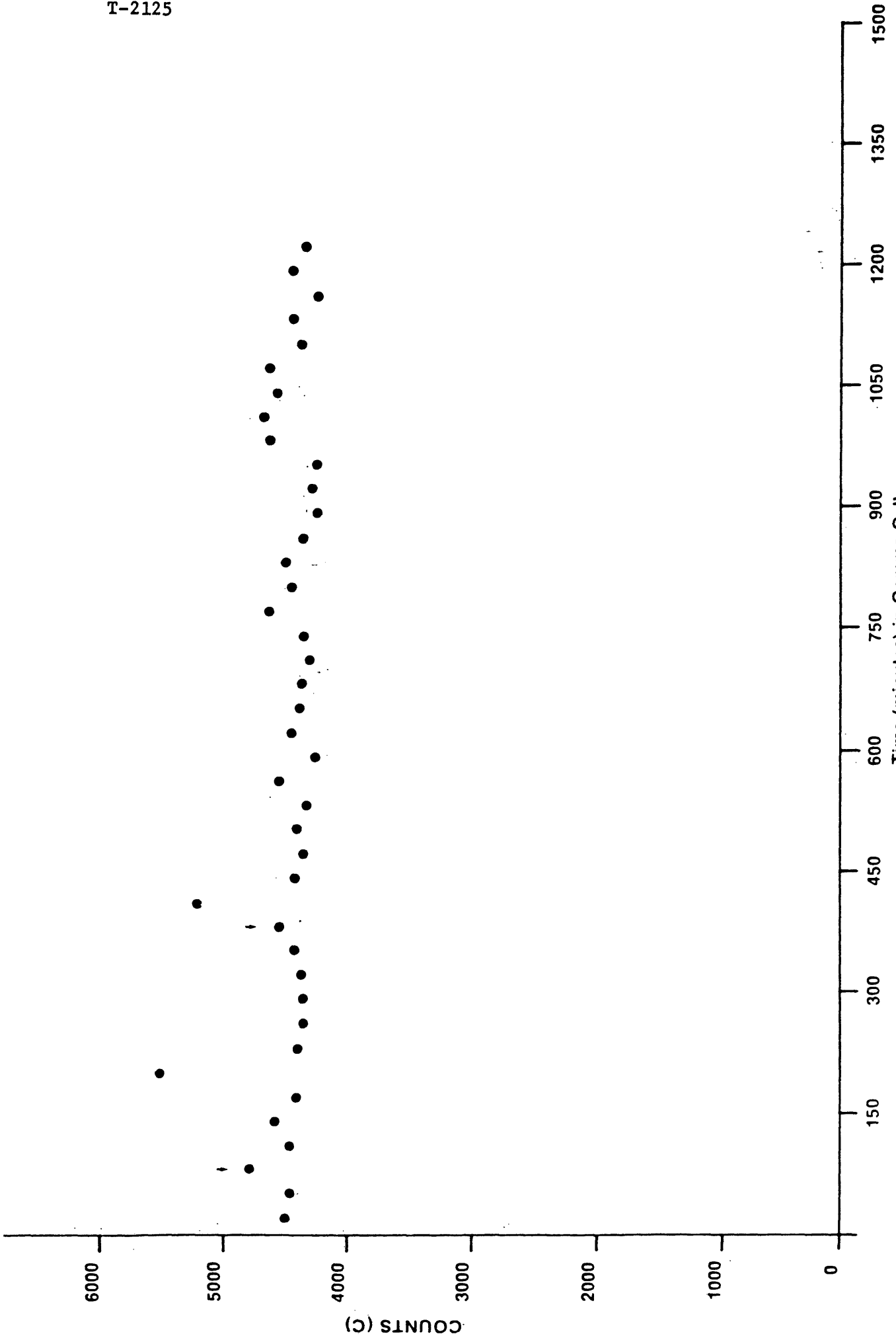


Figure 14 - H₂O + M₀O₂ (run #121)

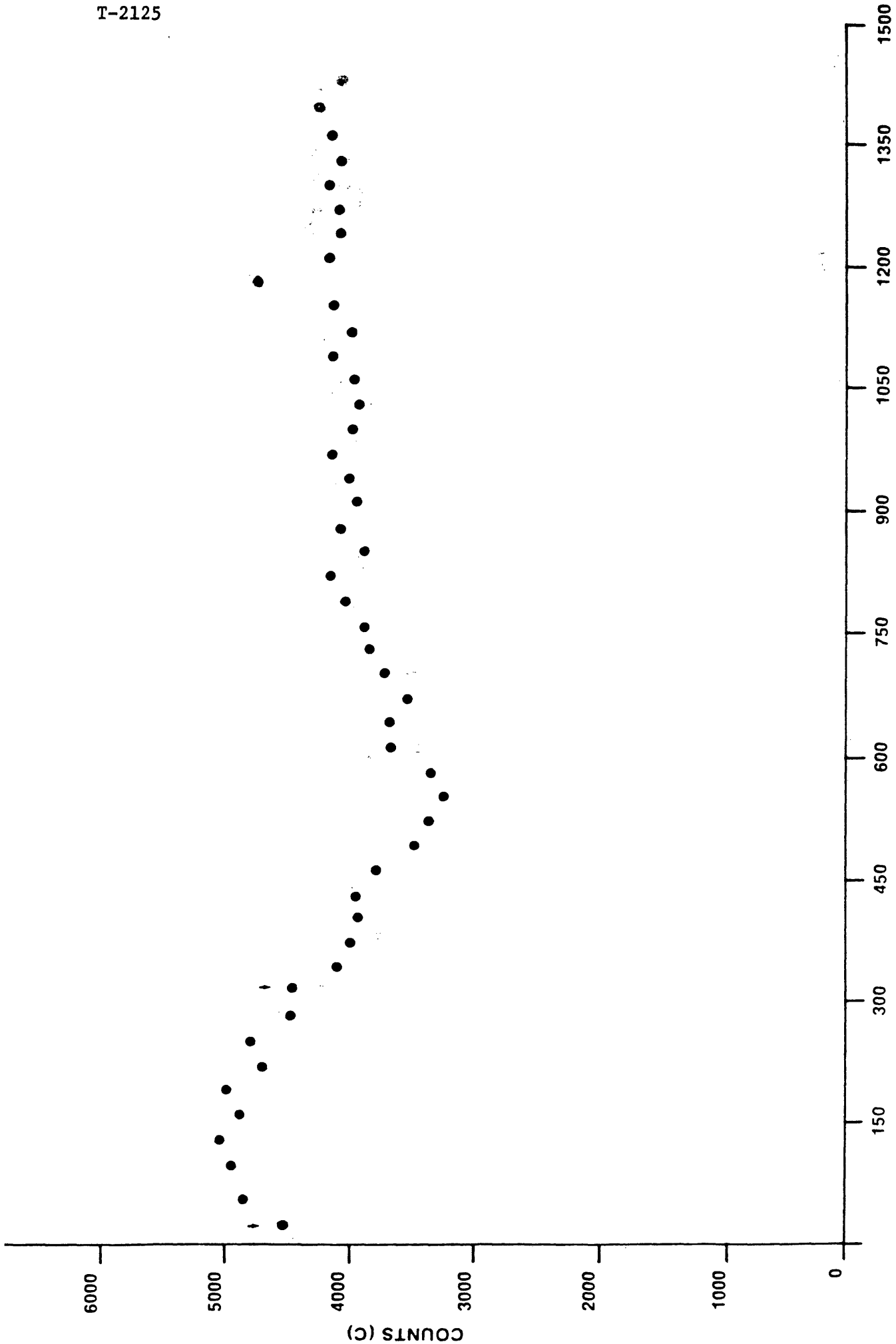


Figure 5— H₂O + In₂O₃ (run #134)

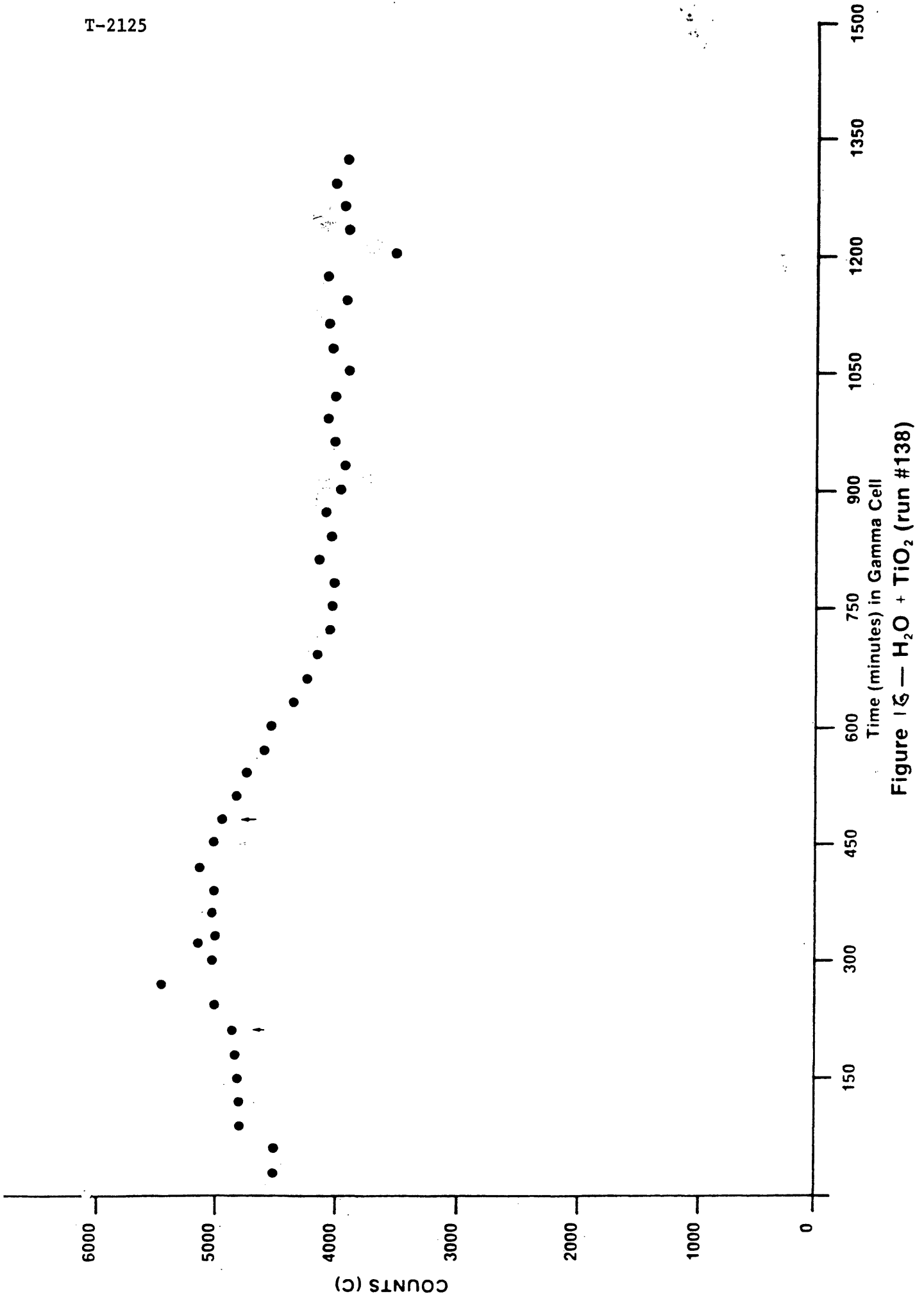


Figure 16 — H₂O + TiO₂ (run #138)

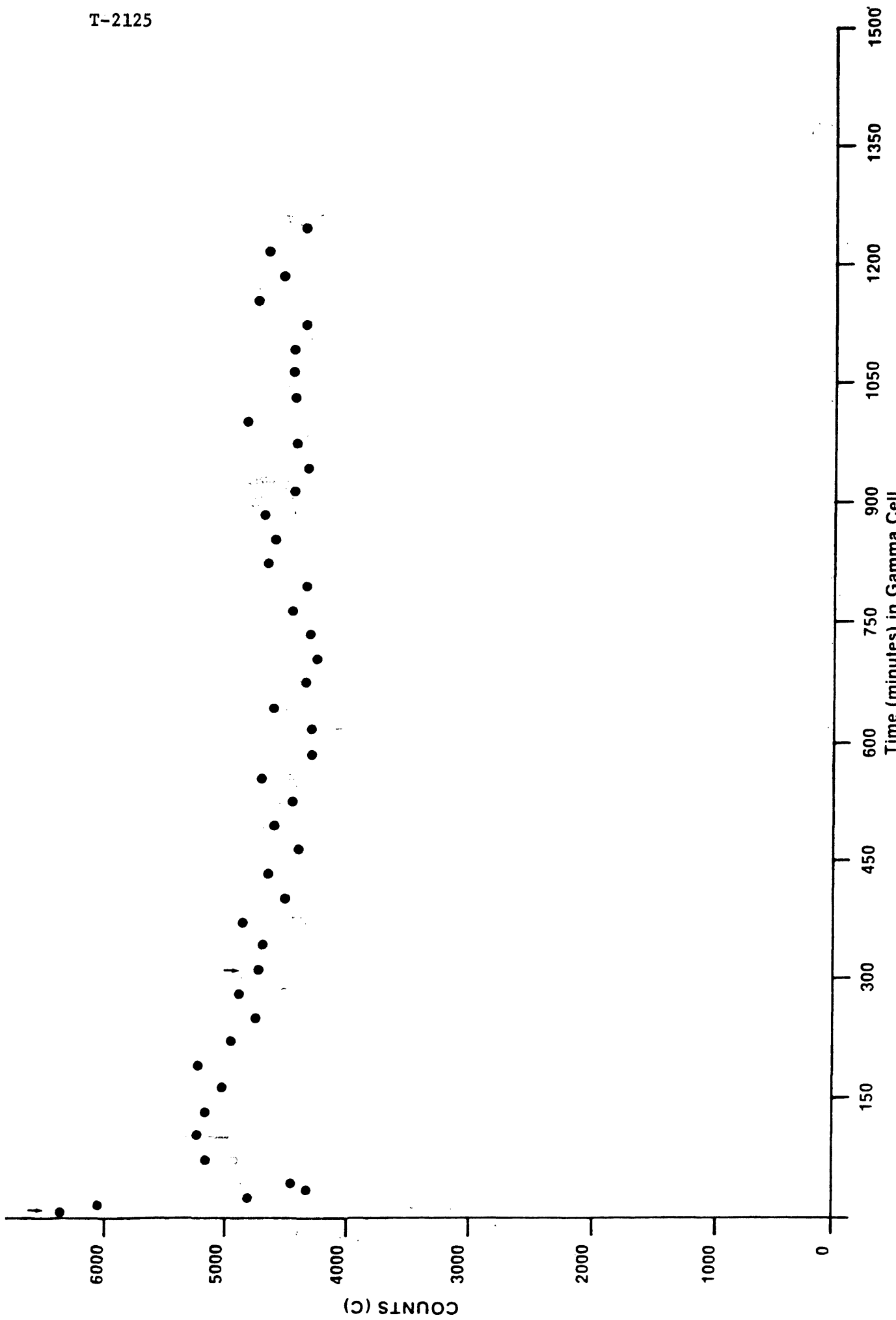


Figure 17 — H₂O + TiO₂ (run #120)

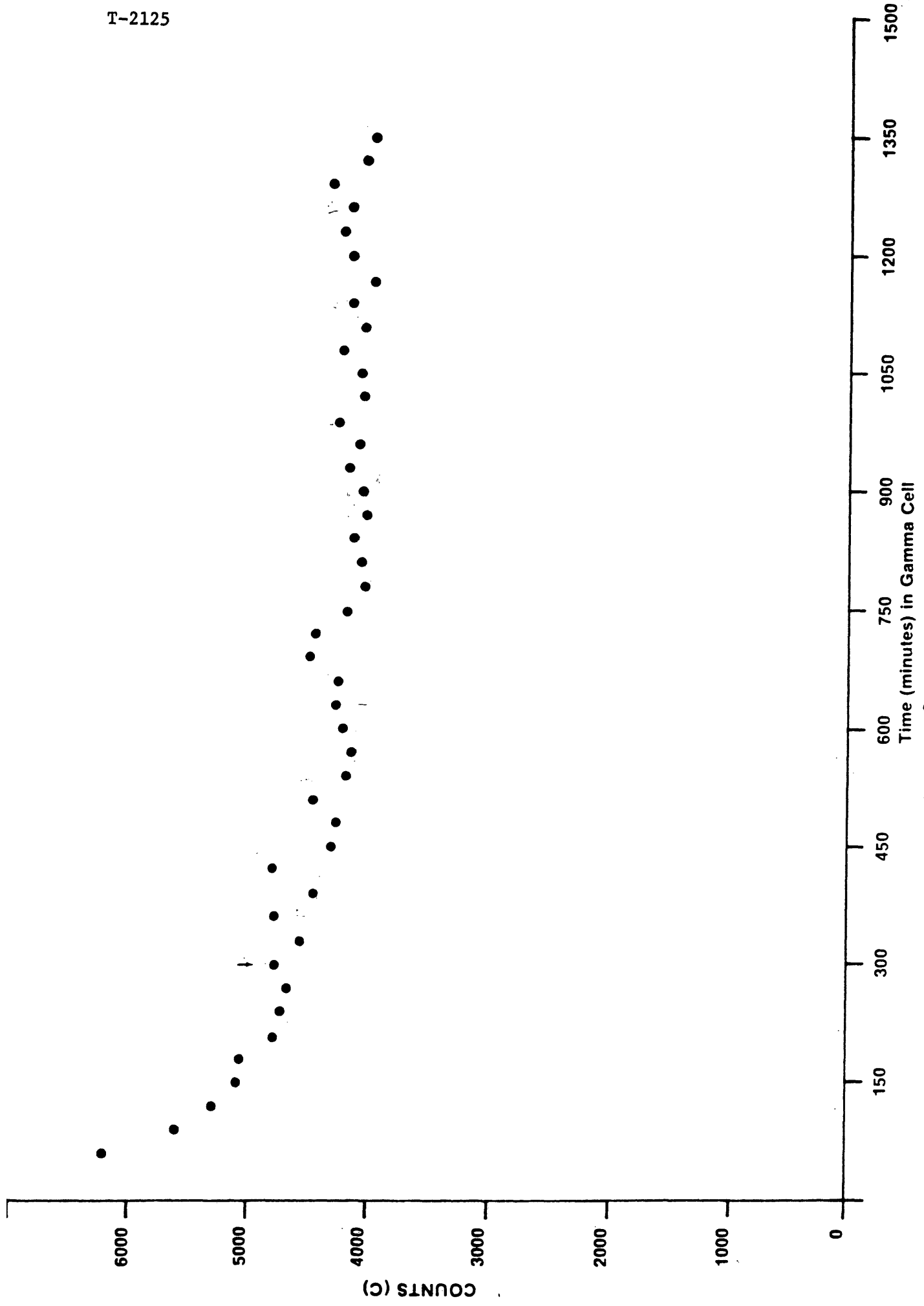


Figure 18 — H₂O + V₂O₅ (run #128)

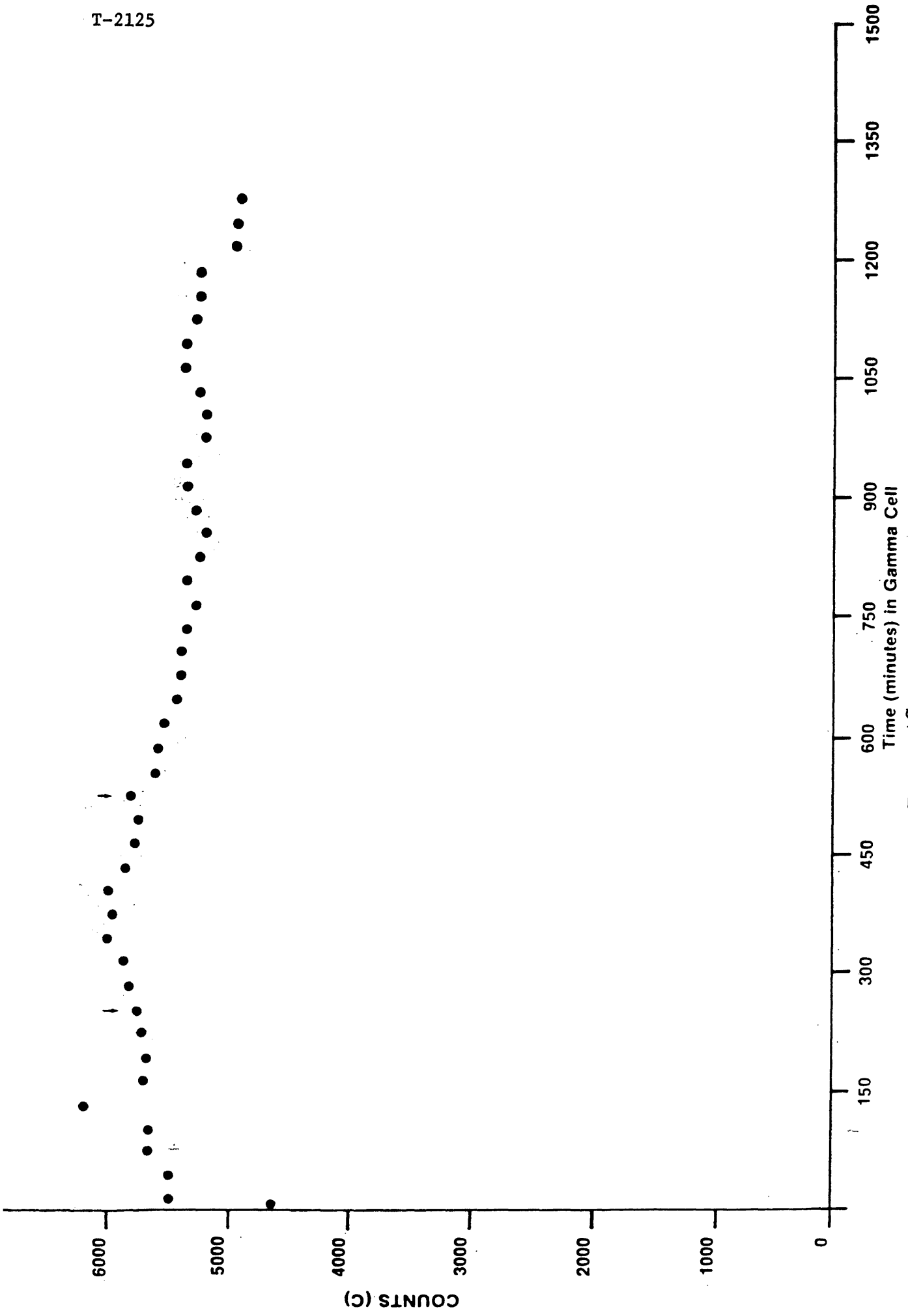


Figure 19 — H₂O + MgO (run #137)

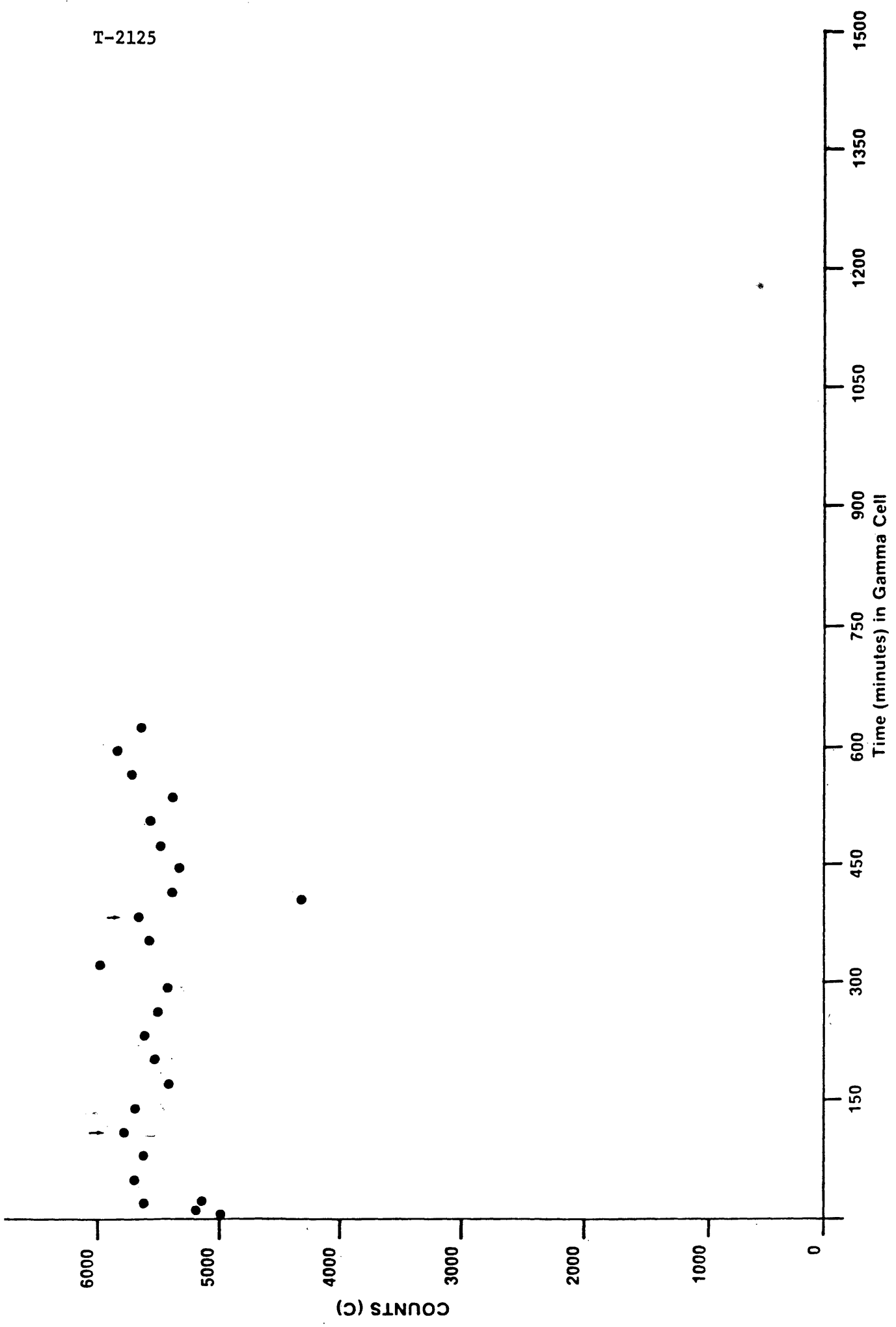


Figure 20 — H₂O + MgO (run #119)

T-2125

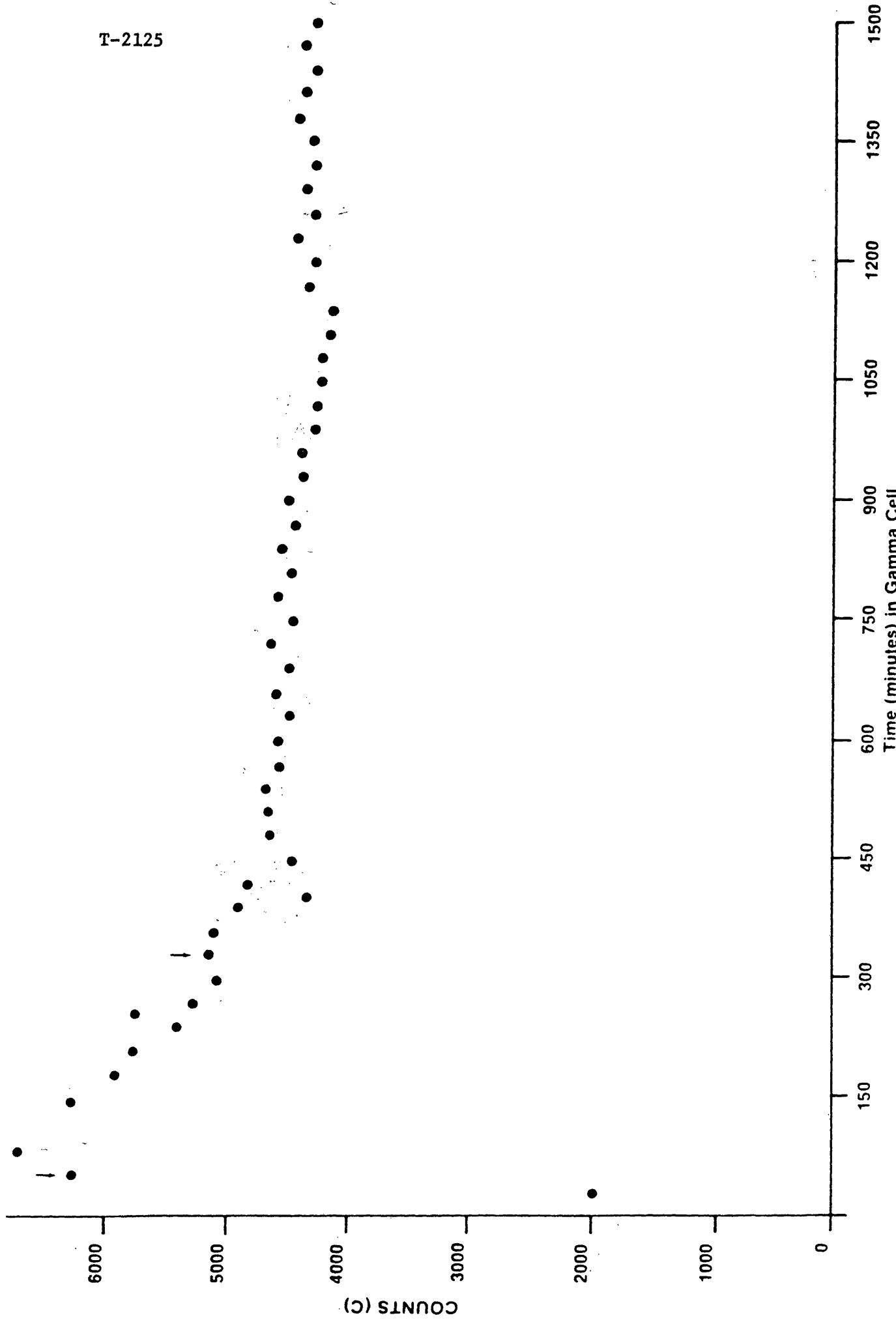


Figure 2f — H₂O + Sb₂O₃ (run #136)

T-2125

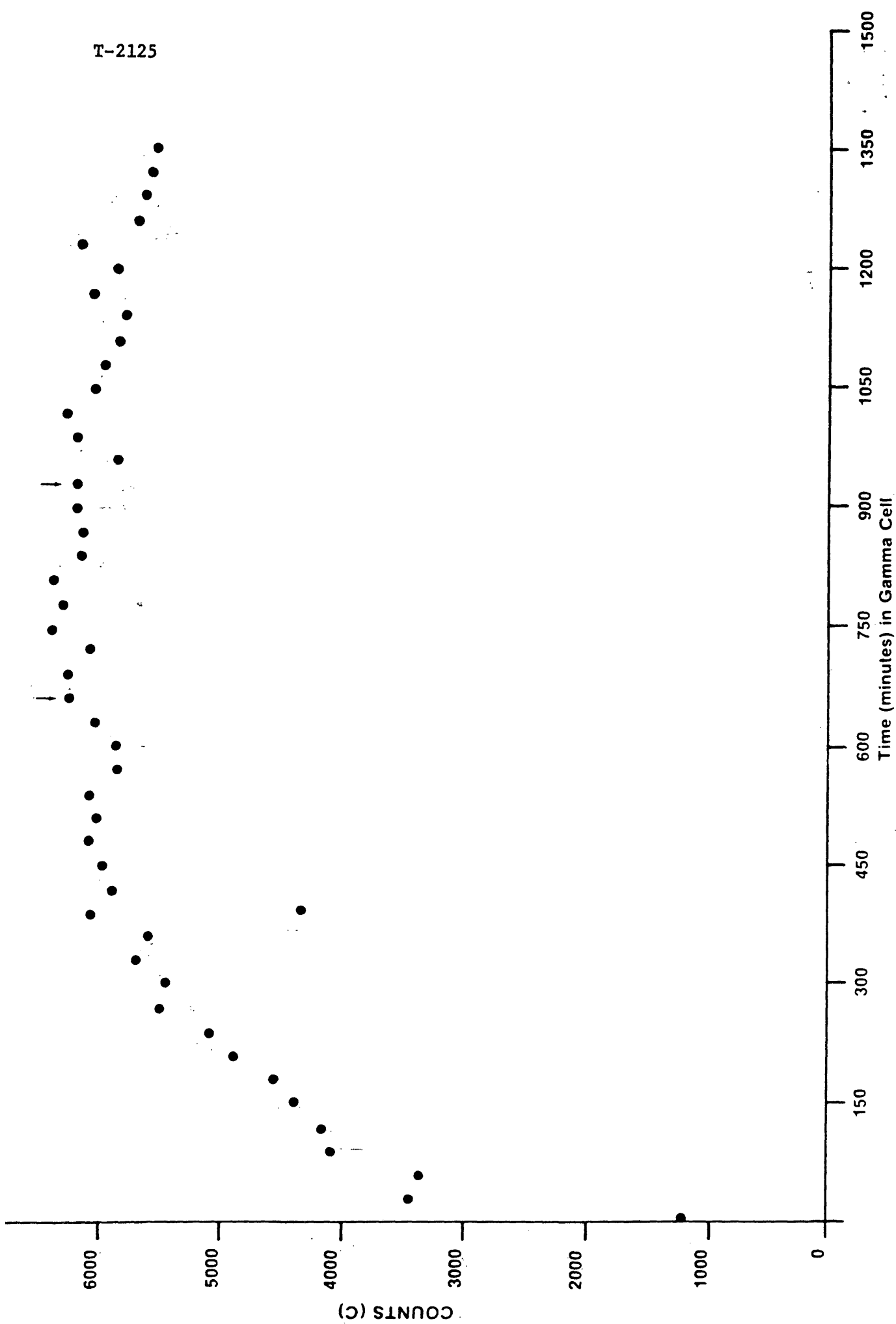


Figure 22 — H₂O + HfO₂ (run #131)

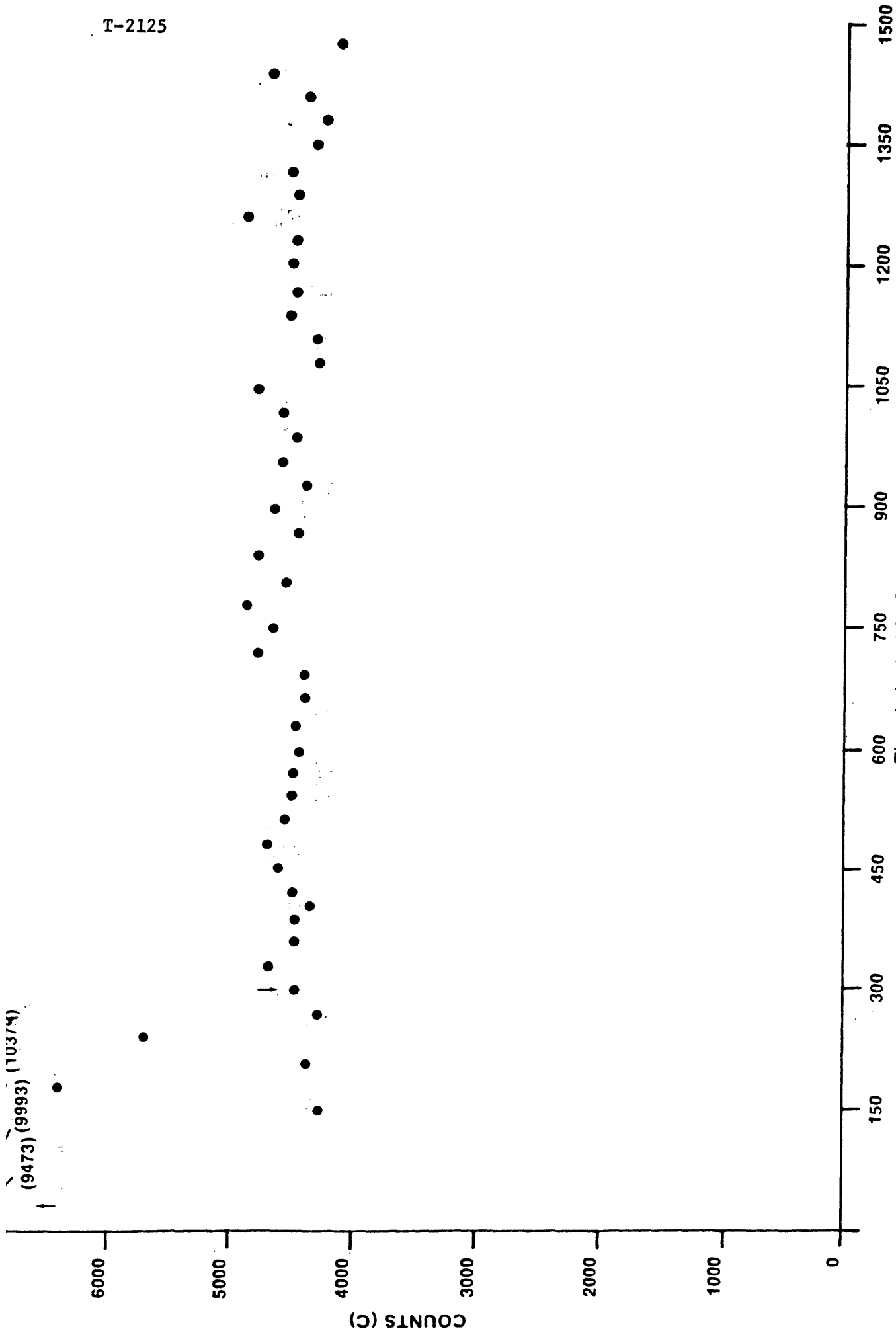


Figure 23 — H₂O + SnO₂ (run # 130)

T-2125

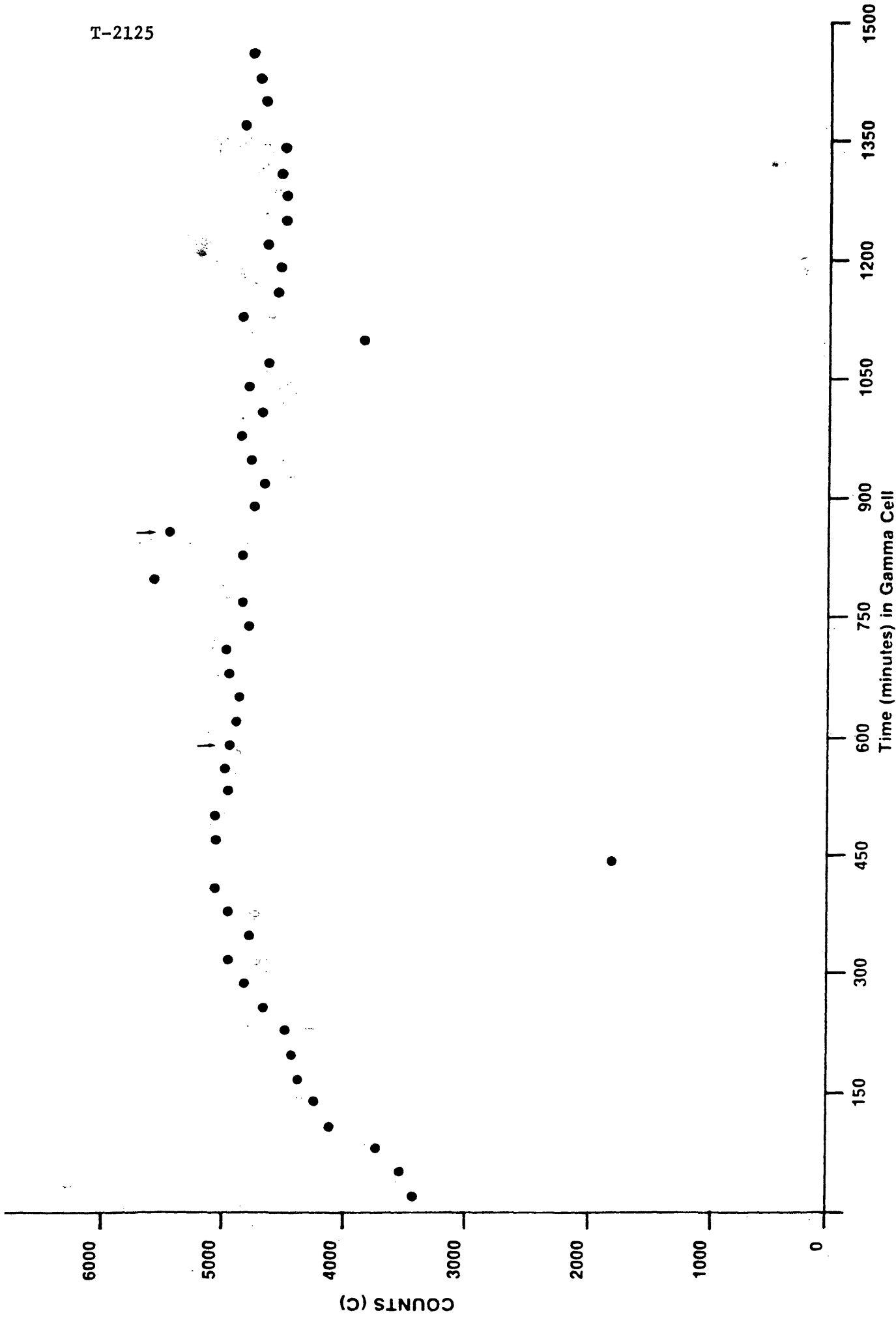


Figure 24 — H₂O (run #139)

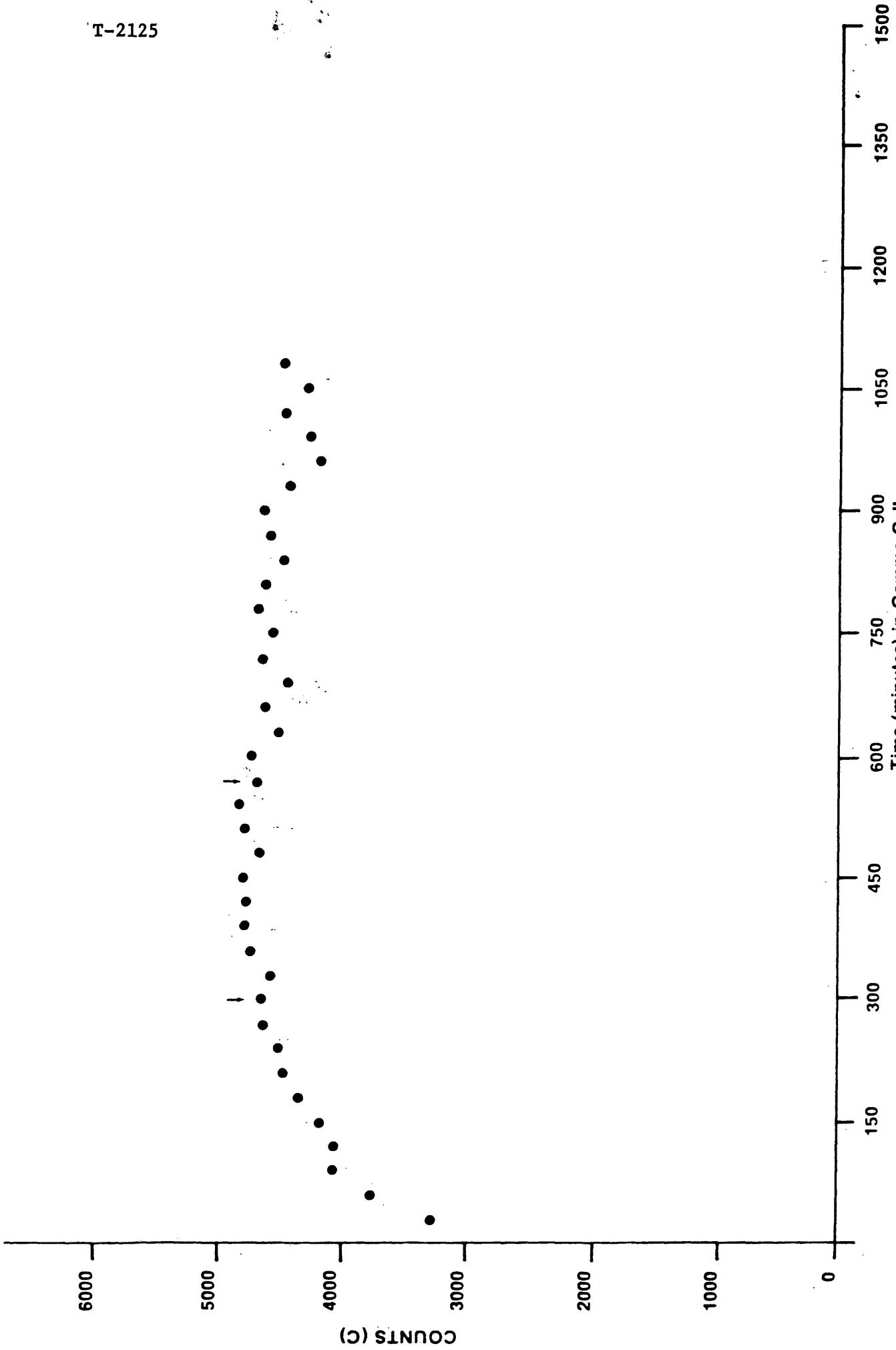


Figure 25 — H₂O (run #132)

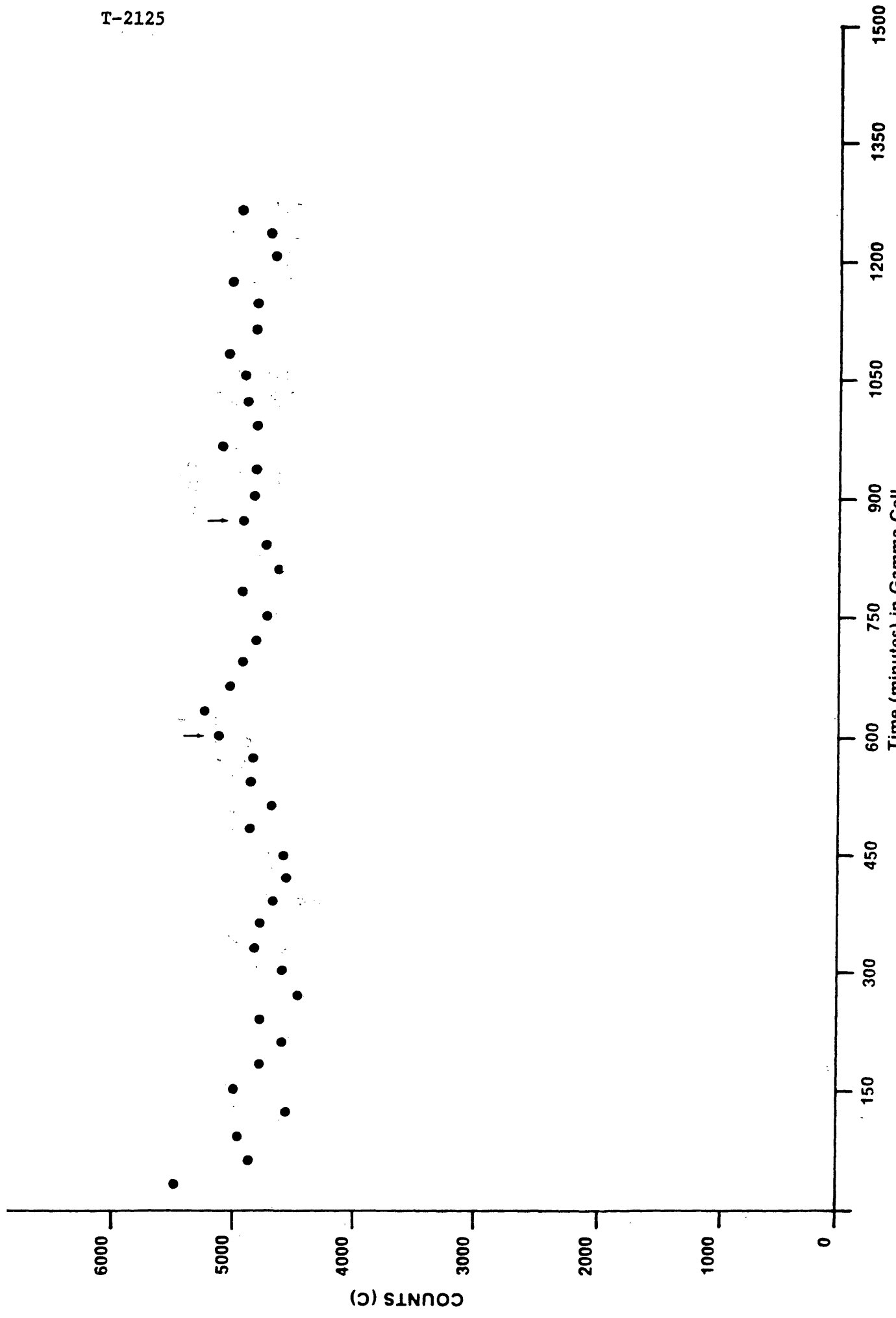


Figure 26— H₂O (run #118)

APPENDIX IITABULATION OF DATA

The following table lists the data used. These values are for an actual transport gas flow rate of 46.3 ± 0.9 cc/min. and a gamma radiation dose rate of $3.12 \pm 0.03 \times 10^5$ rads/hr.

Table 9. Experimental Data

<u>RUN NUMBER</u>	<u>DATE</u>	<u>CATALYST</u>	<u>GRAMS CATALYST</u>	<u>TIME ELAPSED SINCE LAST SAMPLE</u>	<u>INTEGRATOR COUNT (C)</u>
118	5/20/78	NONE	---	30	5451
				30	4855
				30	4942
				30	4529
				30	4998
				30	4745
				30	4582
				30	4744
				30	4451
				30	4570
				30	4811
				30	4770
				30	4667
				30	4546
				30	4594
				30	4864
				30	4690
				30	4876
				30	4820
				30	5118
				30	5231
				30	5060
				30	4912
				30	4803
				30	4725
				30	4948
				30	4649
				30	4715
				30	4922
				30	4840
				30	4822
				30	5129
				30	4813
				30	4900
				30	4908
				30	5087
				30	4804
				30	4814
				30	5054
				30	4698
				30	4710
				30	4980

RUN NUMBER	DATE	CATALYST	GRAMS CATALYST	TIME ELAPSED SINCE LAST SAMPLE	INTEGRATOR COUNT (C)
119	5/21/78	MgO	0.75	6	740
				6	4970
				5	5152
				5	5114
				5	5590
				30	5671
				30	5597
				30	5746
				30	5645
				30	5391
				30	5496
				30	5587
				30	5459
				30	5390
				30	5951
				30	5510
				30	5608
				30	5339
				30	5271
				30	5456
				30	5607
				30	5344
				30	5700
				30	5807
				30	5605

RUN NUMBER	DATE	CATALYST	GRAMS CATALYST	TIME ELAPSED SINCE LAST SAMPLE	INTEGRATOR COUNT (C)
120	5/22/78	TiO ₂	0.75	7	1875
				5	6377
				8	6064
				9	4821
				10	4380
				6	4472
				30	5156
				30	5244
				30	5178
				30	5029
				30	5222
				30	4953
				30	4765
				30	4897
				30	4726
				30	4699
				30	4879
				30	4507
				30	4678
				30	4414
				30	4622
				30	4474
				30	4735
				30	4317
				30	4301
				30	4656
				30	4373
				30	4291
				30	4337
				30	4488
				30	4367
				30	4676
				30	4606
				30	4699
				30	4487
				30	4334
				30	4445
				30	4854
				30	4455
				30	4470
				30	4482
				30	4348
				30	4765
				30	4547
				30	4676
				30	4377

RUN NUMBER	DATE	CATALYST	GRAMS CATALYST	TIME ELAPSED SINCE LAST SAMPLE	INTEGRATOR COUNT (C)
121	5/23/78	MoO ₃	0.75	30	4461
				30	4430
				30	4785
				30	4412
				30	4556
				30	4370
				30	5487
				30	4485
				30	4435
				30	4428
				30	4436
				30	4500
				30	4638
				30	5197
				30	4405
				30	4322
				30	4296
				30	4372
				30	4387
				30	4301
				30	4528
				30	4235
				30	4420
				30	4380
				30	4366
				30	4299
				30	4336
				30	4620
				30	4452
				30	4598
				30	4448
				30	4212
				30	4293
				30	4221
				30	4609
				30	4686
				30	4575
				30	4606
				30	4395
				30	4529
				30	4335
				30	4434
				30	4236
				30	4559
				30	4449

RUN NUMBER	DATE	CATALYST	GRAMS CATALYST	TIME ELAPSED SINCE LAST SAMPLE	INTEGRATOR COUNT (C)
127	5/29/78	MoO ₃	0.75	30	5018
				30	4946
				30	4834
				30	4543
				30	4659
				30	4480
				30	4423
				30	4306
				30	4421
				30	4608
				30	4505
				30	4511
				30	4477
				30	4559
				30	4447
				30	4478
				30	4284
				30	4458
				30	4284
				30	4316
				30	4218
				30	4113
				30	4092
				30	4239
				30	4062
				30	4049
				30	4125
				30	4154
				30	4055
				30	4183
				30	4025
				30	4183
				30	4148
				30	4192
				30	4227
				30	4349
				30	4228
				30	4382
				30	4199
				30	4413
				30	4367
				30	4375
				30	4173
				30	4210
				30	4283
				30	4252
				30	4275
				30	4050
				30	4181
				30	4197

RUN NUMBER	DATE	CATALYST	GRAMS CATALYST	TIME ELAPSED SINCE LAST SAMPLE	INTEGRATOR COUNT (C)
128	5/30/78	V ₂ O ₅	0.75	30	7447
				30	6177
				30	5589
				30	5256
				30	5064
				30	5023
				30	4730
				30	4697
				30	4638
				30	4734
				30	4515
				30	4767
				30	4400
				30	4775
				30	4290
				30	4244
				30	4425
				30	4163
				30	4109
				30	4188
				30	4264
				30	4227
				30	4476
				30	4420
				30	4157
				30	4017
				30	4145
				30	4109
				30	4006
				30	4050
				30	4186
				30	4083
				30	4259
				30	4042
				30	4065
				30	4206
				30	4040
				30	4124
				30	3958
				30	4165
				30	4234
				30	4180
				30	4321
				30	4024
				30	3978

<u>RUN</u> <u>NUMBER</u>	<u>DATE</u>	<u>CATALYST</u>	<u>GRAMS</u> <u>CATALYST</u>	<u>TIME ELAPSED</u> <u>SINCE LAST SAMPLE</u>	<u>INTEGRATOR COUNT</u> <u>(C)</u>
130	6/1/78	SnO ₂	0.75	30	9473
				30	9993
				30	10379
				30	7524
				30	4223
				30	6365
				30	4324
				30	5667
				30	4258
				30	4430
				30	4678
				30	4417
				30	4457
				30	4469
				30	4573
				30	4674
				30	4509
				30	4479
				30	4469
				30	4433
				30	4421
				30	4375
				30	4399
				30	4777
				30	4610
				30	4745
				30	4606
				30	4826
				30	4495
				30	4734
				30	4417
				30	4661
				30	4365
				30	4587
				30	4434
				30	4595
				30	4766
				30	4259
				30	4298
				30	4494
				30	4446
				30	4487
				30	4442
				30	4821
				30	4417
				30	4495
				30	4289
				30	4218
				30	4352
				30	4625
				30	4094

RUN NUMBER	DATE	CATALYST	GRAMS CATALYST	TIME ELASPED SINCE LAST SAMPLE	INTEGRATOR COUNT (C)
131	6/2/78	HfO ₂	0.75	7	1175
				30	3435
				30	3331
				30	4064
				30	4131
				30	4395
				30	4526
				30	4898
				30	5072
				30	5474
				30	5406
				30	5692
				30	5580
				30	6039
				30	5884
				30	5931
				30	6070
				30	6002
				30	6078
				30	5836
				30	5867
				30	6015
				30	6250
				30	6250
				30	6086
				30	6371
				30	6294
				30	6377
				30	6110
				30	6104
				30	6185
				30	6192
				30	5827
				30	6176
				30	6288
				30	6011
				30	5957
				30	5838
				30	5792
				30	6043
				30	5862
				30	6167
				30	5697
				30	5601
				30	5584
				30	5531

RUN NUMBER	DATE	CATALYST	GRAMS CATALYST	TIME ELAPSED SINCE LAST SAMPLE	INTEGRATOR COUNT (C)
132	6/3/78	NONE	---	30	3241
				30	3722
				30	4048
				30	4019
				30	4161
				30	4306
				30	4452
				30	4476
				30	4606
				30	4604
				30	4568
				30	4713
				30	4753
				30	4739
				30	4775
				30	4638
				30	4767
				30	4828
				30	4682
				30	4729
				30	4502
				30	4612
				30	4428
				30	4649
				30	4506
				30	4631
				30	4587
				30	4690
				30	4608
				30	4489
				30	4579
				30	4614
				30	4435
				30	4177
				30	4263
				30	4477
				30	4282
				30	4244
				30	4487

RUN NUMBER	DATE	CATALYST	GRAMS CATALYST	TIME ELAPSED SINCE LAST SAMPLE	INTEGRATOR COUNT (C)
134	6/5/78	In ₂ O ₃	0.75	5	930
				30	4515
				30	4817
				30	4923
				30	5022
				30	4877
				30	4948
				30	4687
				30	4783
				30	4449
				30	4407
				30	4077
				30	3980
				30	3906
				30	3922
				30	3760
				30	3462
				30	3369
				30	3233
				30	3347
				30	3643
				30	3676
				30	3501
				30	3722
				30	3838
				30	3866
				30	4017
				30	4160
				30	3884
				30	4048
				30	3902
				30	3984
				30	4107
				30	3996
				30	3906
				30	3962
				30	4132
				30	3977
				30	4131
				30	4939
				30	4186
				30	4055
				30	4072
				30	4139
				30	4061
				30	4144
				30	4228
				30	4083

RUN NUMBER	DATE	CATALYST	GRAMS CATALYST	TIME ELAPSED SINCE LAST SAMPLE	INTEGRATOR COUNT (C)
136	6/7/78	Sb ₂ O ₃	0.75	30	1940
				30	6222
				30	6674
				30	7001
				30	6226
				30	5897
				30	5728
				30	5383
				30	5222
				30	5052
				30	5102
				30	5093
				30	4869
				30	4800
				30	4440
				30	4603
				30	4618
				30	4647
				30	4543
				30	4550
				30	4471
				30	4582
				30	4477
				30	4612
				30	4464
				30	4585
				30	4461
				30	4530
				30	4425
				30	4492
				30	4383
				30	4378
				30	4393
				30	4272
				30	4264
				30	4207
				30	4215
				30	4147
				30	4113
				30	4307
				30	4293
				30	4436
				30	4277
				30	4330
				30	4274
				30	4299
				30	4410
				30	4350
				30	4350
				30	4269
				30	4372
				30	4258

RUN NUMBER	DATE	CATALYST	GRAMS CATALYST	TIME ELASPED SINCE LAST SAMPLE	INTEGRATOR COUNT (C)
137	6/8/78	MgO	0.25	5	474
				6	4604
				7	5485
				30	5478
				30	5627
				30	5606
				30	6182
				30	5681
				30	5648
				30	5687
				30	5712
				30	5796
				30	5807
				30	5978
				30	5918
				30	5965
				30	5818
				30	5748
				30	5715
				30	5785
				30	5595
				30	5581
				30	5500
				30	5406
				30	5399
				30	5385
				30	5336
				30	5253
				30	5304
				30	5234
				30	5194
				30	5250
				30	5306
				30	5317
				30	5186
				30	5182
				30	5237
				30	5350
				30	5357
				30	5261
				30	5216
				30	5216
				30	4945
				30	4949
				30	4908

<u>RUN</u> <u>NUMBER</u>	<u>DATE</u>	<u>CATALYST</u>	<u>GRAMS</u> <u>CATALYST</u>	<u>TIME ELAPSED</u> <u>SINCE LAST SAMPLE</u>	<u>INTEGRATOR COUNT</u> <u>(C)</u>
138	6/9/78	T ₂ O ₂	0.75	7	1386
				7	6076
				30	4523
				30	4539
				30	4823
				30	4828
				30	4829
				30	4864
				30	4898
				30	5027
				30	5470
				30	5063
				30	5022
				30	5051
				30	5018
				30	5150
				30	5046
				30	4980
				30	4849
				30	4759
				30	4600
				30	4564
				30	4393
				30	4284
				30	4184
				30	4075
				30	4048
				30	4012
				30	4165
				30	4052
				30	4100
				30	3995
				30	3939
				30	4030
				30	4082
				30	4005
				30	3901
				30	4048
				30	4068
				30	3933
				30	4075
				30	3509
				30	3903
				30	3936
				30	4015
				30	3903

RUN NUMBER	DATE	CATALYST	GRAMS CATALYST	TIME ELAPSED SINCE LAST SAMPLE	INTEGRATOR COUNT (C)
139	6/10/78	NONE	---	30	3413
				30	3539
				30	3726
				30	4116
				30	4230
				30	4395
				30	4413
				30	4484
				30	4685
				30	4813
				30	4943
				30	4788
				30	4947
				30	5061
				30	1800
				30	5047
				30	5052
				30	4934
				30	4971
				30	4926
				30	4894
				30	4882
				30	4936
				30	4978
				30	4776
				30	4840
				30	5576
				30	4836
				30	5434
				30	4721
				30	4685
				30	4765
				30	4765
				30	4825
				30	4672
				30	4794
				30	4604
				30	3821
				30	4840
				30	4544
				30	4533
				30	4638
				30	4497
				30	4489
				30	4521
				30	4497
				30	4814
				30	4634
				30	4695
				30	4719

BIBLIOGRAPHY

1. O.V. Krylov, "Special Features of Catalysis On Magnesium Oxide and Oxide-Dielectrics Which are Close To It." Problemy Kinctiki i Kataliza XV, Mekhanizm i Kinetika Geterogenngkh Reaktsiy, Izd vo Nauka, Moscow, 1973, pp. 85-94. Translation, AD/A-000 186, Foreign Technology Division, Wright-Patterson Air Force Base, Ohio, 4 October 1974.
2. R. Coekelbergs, A. Cruz and A. Frennet, "Advances In Catalysis", Vol. 13 p. 55, Academic Press, New York, 1962.
3. D.G. Klissurski, "On the Approximate Correlation Between The Bonding Energy of Oxygen In Metal Oxides And The Width Of Their Forbidden Zones", Solid State Comm., Vol. 15, pp. 1789-1792 (1974).
4. J.G. Morse, Unpublished research paper, 1976.
5. Y.K. Sgrkin and M.E. Dyatkina, "Structure Of Molecules And The Chemical Bond", Dover Publications, Inc., New York, 1964.
6. W.H. Strehlow and E.L. Cook, "Compilation Of Energy Band Gaps In Elemental And Binary Compound Semiconductors And Insulators", J. Phys. Chem. Ref. Data, Volume 2, No 1, pp. 163-169, 1973.
7. Z.O. Draganic and I.G. Draganic." Radiation Chemistry of Water", Academic Press, New York, 1971.
8. M. Burton and J. Magee, "Advances In Radiation Chemistry", John Wiley and Sons, Inc., New York, 1969.
9. A.O. Allen, "Radiation Chemistry Of Water And Aqucous Solutions", D. Van Nostrand.
10. J.W.T. Spinks and R.J. Woods, "An Introduction To Radiation Chemistry", John Wiley and Sons, 1976.

11. C. Kittel, "Introduction to Solid State Physics", John Wiley and Sons, Inc, New York, 1971.
12. J.S. Blakemore, "Solid State Physics", W.B. Saunders Company, Philadelphia, PA, 1974.
13. F.F. Volkenshtein, "The Electronic Theory of Catalysis on Semiconductors", MacMillan Company, New York, New York, 1963.
14. M. Prettre, "Catalysis and Catalysts", Dover Publications, Inc, New York, New York, 1963.